scientific reports

Check for updates

OPEN

Vitamin D₃ reduces the expression of M1 and M2 macrophage markers in breast cancer patients

Martyna Stachowicz-Suhs[1], Natalia Łabędź[1], Magdalena Milczarek[1], Dagmara Kłopotowska[1], Beata Filip-Psurska[1], Adam Maciejczyk[2,3], Rafał Matkowski[2,3] & Joanna Wietrzyk[1]✉

Vitamin D₃ (VD) is known for its immunomodulatory and anticancer effects. This study aimed to characterize tumor-associated macrophages (TAMs) in breast cancer (BC) and assess the influence of VD and its active metabolite, calcitriol, on their polarization. TAMs were isolated from BC patients and characterized. Monocytes were differentiated into macrophage classes (M0, M1, M2a, M2c) and treated ex vivo with calcitriol. The expression of VD-related proteins in tumor tissue was correlated with TAMs and monocyte-derived macrophages (MDMs) characteristics. TAM expression of CD200R, CD204, CD80, HLA-DR, and CD44 was negatively correlated with CYP27B1 in selected patient groups. Patients with high CYP27B1 tumor expression showed significantly lower CD200R, CD204, and CD44 expression. In patients with normal VD levels and premenopausal, CD80 expression in M2a and M2c MDMs (control, untreated ex vivo with calcitriol) was negatively correlated with plasma VD. Calcitriol reduced HLA-DR during MDM differentiation in all patients; CD80 decrease significantly except in patients with normal VD levels or metastasis. Calcitriol also decreased CD163 expression. The decrease in both M1 and M2 macrophage markers by calcitriol or their negative correlation with CYP27B1 indicate the modulatory, but rather anticancer activity of VD. The intensity of these effects was the strongest in postmenopausal patients and those without metastases.

Keywords Vitamin D₃, Calcitriol, Breast cancer, TAMs, Macrophages

Abbreviations

BC	breast cancer
COX-2	cyclooxygenase 2
VD	vitamin D₃
CYP24A1	24-Hydroxylase
CYP27B1	1-a-Hydroxylase
EGF	epidermal growth factor
EMT	epithelial–mesenchymal transition
EpCAM	epithelial cell adhesion molecule antigen
ER	estrogen receptor
FSH	follicle-stimulating hormone
HER2	human epidermal growth factor receptor
INF	interferon
IRF4	interferon regulatory factor 4
LPS	lipopolysaccharide
M-CSF	macrophage colony-stimulating factor
MDMs	monocyte-derived macrophages
MMP-3	metalloproteinase 3
OPN	osteopontin
PGE2	prostaglandin E2
PR	progesterone receptor
PTH	parathyroid hormone

[1]Department of Experimental Oncology, Hirszfeld Institute of Immunology and Experimental Therapy, Wroclaw, Poland. [2]Department of Oncology, Wrocław Medical University, Wrocław, Poland. [3]Lower Silesian Oncology, Pulmonology and Hematology Center, Wrocław, Poland. ✉email: joanna.wietrzyk@hirszfeld.pl

PTHLH	parathyroid hormone-like hormone
S100A8	S100 calcium-binding protein A8
TAMs	tumor-associated macrophages
TGFβ	transforming growth factor β
TME	tumor microenvironment
VDR	vitamin D receptor
VEGF	vascular endothelial growth factor
ViDA	Vitamin D Assessment
VITAL	Vitamin D and Omega-3 Trial
ZEB-1	proteins from the E-Box zinc finger family binding homeobox 1

Vitamin D_3 (VD) is renowned for its immunomodulatory effects, and its potential to lower the risk of various cancers, including breast cancer, has been widely discussed. Numerous studies have explored the mechanisms underlying its anticancer properties[1,2].

Epidemiological studies have suggested a lower risk of breast cancer in women with high serum $25(OH)D_3$ (a VD metabolite) concentrations (≥ 45 ng/mL) compared to those with low serum $25(OH)D_3$ concentrations, particularly when measured in the summer. However, overall analyses have not consistently shown statistically significant correlations[3]. Other studies have highlighted the significant impact of high $25(OH)D_3$ concentrations on reducing mortality[4] and lowering the risk of breast cancer[5]. Studies have also shown that low VD levels were correlated with worse prognostic parameters in postmenopausal patients[6] and are linked to an increased risk of disease regardless of menopausal status[7]. However, findings from clinical trials have not uniformly supported observations from epidemiological studies.

Clinical trials have indicated that VD supplementation (approximately 24 μg/day) does not reduce the risk of breast cancer by more than 30%[8]. Moreover, in another study, daily doses of 400 IU of VD (10 μg) and 1000 mg of calcium carbonate did not significantly reduce the risk of breast cancer or other invasive cancers[9]. The VITAL (Vitamin D and Omega-3 Trial) study, involving 25,871 participants over 55 years of age who were expected to receive a daily dose of 2,000 IU of VD (50 μg), did not show any effect of supplementation on reducing the risk of developing breast cancer or other diseases. However, the cancer mortality rate (total) was significantly lower in the group receiving VD than in the group receiving placebo after 5 years of observation[10]. The ViDA (Vitamin D Assessment) clinical trial, which used monthly doses of 100,000 IU (2,500 μg) of VD, did not show any effect of supplementation on reducing the risk of cancer[11]. Similar results were reported from the Finnish Vitamin D Trial, with the authors suggesting that the lack of effect of supplementation may be attributed to the normal plasma $25(OH)D_3$ concentration among study participants before supplementation[12].

Calcitriol, an active VD metabolite, and key molecules in its biological function, such as the vitamin D receptor (VDR) and enzymes like 24-hydroxylase (CYP24A1) and 1-α-hydroxylase (CYP27B1), play crucial roles in various cellular processes, including proliferation, apoptosis, epithelial–mesenchymal transition, and cancer stem cell formation[13–16]. Many studies have shown that low levels of VDR are associated with a more aggressive type of breast cancer[17,18]. Additionally, its reduction is associated with neoplastic transformation, which decreases the sensitivity of cancer cells to the antiproliferative activity of calcitriol[16,19,20]. For instance, in a mouse mammary gland cancer model (186FARN), silencing the *Vdr* gene accelerated tumor growth and promoted metastasis[21]. Breast cancer cells, irrespective of their estrogen receptor status, express CYP24A1 and CYP27B1, which are responsible for the metabolism of VD[14]. Cancer cells often exhibit increased CYP24A1 levels (which degrade calcitriol) and decreased CYP27B1 levels (which synthesize calcitriol), leading to a reduction in local calcitriol concentrations within the tumor microenvironment[15,16,22]. The dependence of the anticancer effect of calcitriol on the CYP27B1 protein was also demonstrated in transgenic mice with inactivation of the *Cyp27b1* gene. Treatment with calcitriol inhibited spontaneous tumor formation in these mice. In contrast, treatment with the biologically inactive VD metabolite, $25(OH)D_3$, did not affect tumor formation or size, highlighting the important function of CYP27B1 in the early stages of carcinogenesis[23].

In the tumor microenvironment (TME), macrophages known as tumor-associated macrophages (TAMs), originate from a population of residual macrophages or are recruited from peripheral blood monocytes[24]. Upon entering the TME, these cells differentiate under the influence of various factors present in the tumor tissue, leading to the classification of macrophages into two main subpopulations, M1 and M2, in a context described as antitumor or protumor[25]. Both human and mouse macrophages express VDR and CYP27B1, enabling them to respond to calcitriol and synthesize it. The factors stimulating the expression of CYP27B1 in macrophages are interferon (INF) γ and lipopolysaccharide (LPS)[26,27]. The metabolism of calcitriol in monocyte-derived macrophages (MDMs) varies depending on the direction of their polarization. Studies have shown that MDMs differentiated into M2a macrophages produce more calcitriol compared to M2c, M1, and M0 MDMs. Additionally, CYP24A1 is responsible for the degradation of calcitriol in these cells[28].

Previous in vivo and ex vivo studies in mouse models of breast cancer showed that calcitriol promotes the differentiation of TAMs towards the M2 phenotype, thereby enhancing lung metastasis of 4T1 mouse breast cancer cells[29–31]. However, the effect of calcitriol on these processes appears to vary depending on the specific type of mouse breast cancer being analyzed[29,32,33]. Consequently, we hypothesized that calcitriol may modulate TAMs differently in breast cancer patients or groups of patients. Given the role of VD in breast cancer and the differentiation of monocyte–macrophages, our study aimed to understand VD's impact on the polarization and differentiation of macrophages in the context of various clinical factors related to breast cancer. To address this we evaluate TAMs characteristic in breast cancer tissue and assess the effect of calcitriol on macrophage differentiation in breast cancer patients. These findings were then compared with plasma levels of $25(OH)D_3$ and the expression levels of VDR, CYP24A1, and CYP27B1 in tumor tissue.

Materials and methods

Patients

For the research conducted on tissues from patients diagnosed at the Lower Silesian Center of Oncology, Pulmonology, and Hematology (February 2019 to December 2020), approval was obtained from the Bioethical Committee at the Medical University in Wrocław, Poland (numbers 603/2018 and 855/2019). Studies were carried out in line with the ethical standards of the national and institutional research committee and with the latest version of the Declaration of Helsinki. Blood and tumor tissue samples were collected from 127 patients with early breast cancer (M0—no distant metastases). Inclusion criteria for these patients in the study were a diagnosis of invasive breast cancer in biopsy (regardless of the stage), qualification for primary surgical treatment, tumor size allowing for the collection of sections for the present study after securing tissue material for routine histopathological examination (tumor size greater than 1 cm), and signing an informed consent to participate. Additionally, blood was collected from 11 patients with generalized (disseminated—M1) breast cancer, meeting the criteria of a biopsy-confirmed diagnosis of invasive metastatic breast cancer and signing an informed consent to participate. Blood and tumor tissue were obtained before chemotherapy as part of routine planning (decision of the multidisciplinary tumor board), followed by surgical resection of the tumor. Table 1 shows the basic characteristics of the 127 M0 patients, further categorized into subgroups. Patients were assigned to normal or deficient $25(OH)D_3$ levels groups based on a plasma level lower or greater than 30 ng/mL. They were also stratified based on menopausal status determined by plasma follicle-stimulating hormone (FSH) levels (FSH > 25.8 mIU/mL postmenopausal and FSH < 25.8 mIU/mL premenopausal). Another analysis categorized patients based on the level of CYP27B1 in their tumors (median CYP27B1/β-actin ratio > or < 0.42—median value) (Table 1). Patients were further divided into groups according to the presence or absence of metastases in sentinel lymph nodes (N+) and the expression of human epidermal growth factor receptor 2 (HER2, as histopathological scoring 0–3) (Table 2), with Table 2 also presenting basic clinical parameters of patients with distant metastases (M1). In the analyzed group of patients, the majority of tumors were estrogen receptor (ER)$^+$ (2 patients were ER$^-$, and the expression was not determined in 3 patients) and progesterone receptor (PR)$^+$ (16 patients were PR$^-$, and the expression was not determined in 5 patients). Therefore, additional analyses of the expression of these receptors were omitted.

Previously, research on biological material from 127 patients with locally advanced breast cancer included an analysis of cancer-associated fibroblasts (CAFs), with some data from these patients also included in a previous paper[34]. Data from 60 patients from this group were included in another publication where cyclooxygenase 2 (COX-2) expression was assessed[33]. These two publications contain data on the expression of CYP24A1, CYP27B1, VDR, osteopontin (OPN), and transforming growth factor (TGF) β, with outliers excluded. Here, these data were subjected to different analyses (e.g., correlations with TAM and MDM characteristics); therefore, Additional file 1: Table S1 provides complete data (median and min–max) without discarding outlier data.

The clinical features of the tumor tissue, including tumor size, estrogen receptor (ER) and progesterone receptor (PR) expression, Ki67 expression, and human epidermal growth factor receptor (HER2) status, are summarized in Additional file 1: Table S1.

Parameter		All patients	25(OH)D₃ concentration			Menopausal status			CYP27B1 expression		
			Normal	Deficient	P	Pre	Post	P	Low	High	P
Age	N	127	38	89		38	89		40	39	
	(years)	60 (31–85)	56 (31–83)	63 (32–85)	0.088	47 (31–70)	66 (44–85)	< 0.0001	57 (32–83)	60 (35–83)	0.318
BMI	N	120	36	84		35	85		37	38	
	(kg/m²)	26.8 (16.5–42.5)	25.6 (16.5–36.1)	27.9 (18.5–42.5)	0.002	23.4 (16.5–40.4)	28.1 (17.2–42.5)	< 0.0001	26.8 (16.5–40.3)	27.0 (17.2–38.0)	0.864
25(OH)D₃	N	127	38	89		38	89		40		
	(ng/mL)	23.2 (2.0–67.7)	39.3 (31.3–67.7)	19.6 (2.0–29.2)	< 0.0001	23.7 (11.5–50.4)	21.5 (2.0–67.7)	0.056	21.1 (7.1–60.1)	23.1 (2.0–42.8)	0.874
FSH	N	126	38	88		38	88		40	38	
	(mIU/mL)	58 (2.4–154)	54.9 (2.5–154)	59.2 (2.4–138)	0.551	6.9 (2.4–82.3)	70 (4–154)	< 0.0001	42.2 (2.4–97.6)	54.1 (2.5–154)	0.460
Estradiol	N	127	38	89		38	89		40	38	
	(pg/mL)	14 (4–617)	15 (4–574)	14 (4–617)	0.848	94 (22–617)	8 (4–40)	< 0.0001	17 (4–617)	14 (4–390)	0.926
PTH	N	127	38	89		38	89		40	39	
	(pg/mL)	30.4 (18–230)	29.0 (18.0–53.7)	32 (18.5–230)	0.007	28.5 (18.5–58.6)	33 (18–230)	0.009	31.1 (18.5–52.8)	29.6 (18.5–62.1)	0.890
Statistical analysis: Mann–Whitney test.											

Table 1. Basic characteristics of all patients and patients stratified according to their $25(OH)D_3$ plasma level, menopausal status, and tumor CYP27B1 level.

Parameter		Nonmetastatic (N0M0)	LN-metastatic ($N+$M0)	P	Distant-metastatic (M1)	P vs. N0M0	P vs. $N+$M0	HER2$^-$	HER2$^+$	P
Age	N	88	32		11			39	81	
	(years)	59.5 (31–85)	60 (36–83)	>0.999	66 (38–75)	0.959	>0.999	57 (44–83)	63 (31–85)	0.516
BMI	N	84	31		11			38	76	
	(kg/m^2)	26.8 (16.5–42.5)	26.8 (20.0–39.5)	>0.999	25.4 (19.6–28.7)	>0.999	0.605	27.9 (16.5–40.4)	26.6 (17.2–42.5)	0.202
25(OH)D$_3$	N	88	32		10			39	81	
	(ng/mL)	23.3 (2–67.7)	23.6 (7.14–60.1)	>0.999	26.3 (9.7–39.6)	>0.999	>0.999	21.5 (7.14–67.7)	23.7 (2–60.1)	0.868
FSH	N	88	31		9			39	80	
	(mIU/mL)	60.8 (2.4–154)	54.8 (6.2–105)	>0.999	59.8 (2.1–96.9)	>0.999	>0.999	65 (3.3–112)	56.4 (2.4–154)	0.348
Estradiol	N	88	32		10			39	81	
	(pg/mL)	14 (4–574)	16.5 (4–617)	>0.999	11 (4–135)	>0.999	>0.999	14 (4–390)	13 (4–617)	0.882
PTH	N	88	32		7			39	81	
	(pg/mL)	29.9 (18–230)	31.2 (18.5–57.4)	>0.999	38.6 (4.6–48.2)	>0.999	>0.999	34.2 (18.5–91.3)	29.6 (18–79.4)	0.090

Table 2. Clinical characteristics of patients stratified according to metastasis* and HER2 status. Statistical analysis: Dunn's multiple comparison tests; *according to TNM classification: N, sentinel lymph node (LN) spread; M, distant metastases.

Isolation and differentiation of monocytes from the peripheral blood of patients

The venous blood of patients was collected in EDTA-S-Monovette tubes (Sarstedt, Nümbrecht, Germany) and centrifuged at 4 °C to obtain plasma for further analysis (-80 °C storage). The remaining blood cells were diluted twice in Hanks' solution (PChO, Wrocław, Poland) and layered onto Ficoll solution (Ficoll Paque Premium-1.073, GE Healthcare, Chicago, Illinois, USA) in 15 mL tubes at room temperature. After centrifugation (400×g for 30 min), the buffy-coat PBMCs were collected. The cells were washed twice by centrifugation in PBS, resuspended in a final volume of 5 mL, and counted. Anti-CD14 antibody conjugated to magnetic beads (Miltenyi Biotec, Auburn, CA, USA) was added to the cells following the manufacturer's recommendations—20 µL of antibody and 80 µL of separation buffer for every 10 million cells. The magnetic separation procedure was conducted. The isolated monocytes were counted and seeded into at least 8 wells of a 12-well plate (Greiner Cell Suspension, Greiner Bio-One, Kremsmünster, Austria) at a concentration of 5×10^5 cells per well in a culture medium (RPMI G.MAX (Thermo Fisher Scientific, Waltham, MA, USA); 5% FBS (Sigma-Aldrich, Saint Louis, MO, USA); 5% horse serum (HS, GIBCO, Thermo Fisher Scientific, Waltham, MA, USA); 4 mM L-glutamine; 2.5 g/L glucose; 1 mM pyruvate; 1% amino acids (Sigma-Aldrich, Saint Louis, MO, USA); 0.1 mg/mL streptomycin and 100 U/mL penicillin (Polfa Tarchomin, Warsaw, Poland)) supplemented with 50 ng/mL human recombinant macrophage colony-stimulating factor (M-CSF) (BioLegend, San Diego, CA, USA). The purity of the isolate was checked using flow cytometry. Monocytes were defined as percentage of double positive cell for CD45-FITC and CD14-BV421 (BioLegend, San Diego, CA, USA). An average purity of the samples was 87.15% ± 13.3 (Additional file 1 Figure S1).

The isolated monocytes were differentiated into macrophages over 7 days using M-CSF (50 ng/mL) with medium exchanges on days 3 and 6. On the eighth day, the macrophages were polarized into individual classes of macrophages (MDMs; monocyte-derived macrophages; details in Fig. 1) without or with calcitriol at three different concentrations of 1, 10, and 100 nM. After 48 h of differentiation into the following macrophage classes: M0 (stimulating factor: M-CSF 50 ng/mL), M1 (stimulating factor: LPS 100 ng/mL, INFγ 50 ng/mL), M2a (stimulating factor: IL-4 50 ng/mL) and M2c (stimulating factor: IL-10 50 ng/mL), cell activation was carried out for 24 h with LPS at a concentration of 100 ng/mL. On day 11, the cells were harvested using Accutase solution (300 µL/well; Merck, Darmstadt, Germany). The cells collected from the individual groups described above were suspended in 1 mL of PBS supplemented with 2% FBS and subjected to cytometric analysis to evaluate the MDMs phenotype. The surface-markers characteristic for macrophages and their subpopulations (M1, M2a and M2c) were tested: CD11b, CD14, (HLA-DR) MHC II (phenotypic M1 marker), CD80 (phenotypic M1 marker), CD163 (phenotypic M2c marker), CD204 (phenotypic M2a marker), CD200R (phenotypic M2c marker), CD44 (phenotypic M2 marker) (Table 3). Data were processed using BD FACSDiva software (version 8.0.2, https://www.bdbiosciences.com/en-pl/products/software/instrument-software/bd-facsdiva-software), following gating on the myeloid cell population in the forward scatter (FSC) and side scatter (SSC) plot. Analysis was restricted to individual cells. The results were reported as the ratio of the median fluorescence intensity (MFI) for the target marker relative to the MFI of unstained controls to monitor changes of MDMs phenotype during the process of differentiation under the influence of calcitriol treatment.

Magnetic separation of TAMs from tumors and monocytes from the peripheral blood of patients

Tumor fragments were preserved in a culture medium solution containing 0.1 mg/mL primocin (InvivoGen, San Diego, CA, USA) and transferred to a sterile Petri dish, with all isolation stages performed on ice. The fragments were mixed with 1 mL of medium (RPMI G.MAX (Thermo Fisher Scientific, Waltham, MA, USA), 5% FBS (Sigma-Aldrich, Saint-Louis, MO, USA), 5% horse serum (HS) serum (GIBCO, Thermo Fisher Scientific, Waltham, MA, USA), 4 mM L-glutamine, 2.5 g/L glucose, 1 mM pyruvate, 1% amino acids (Sigma-
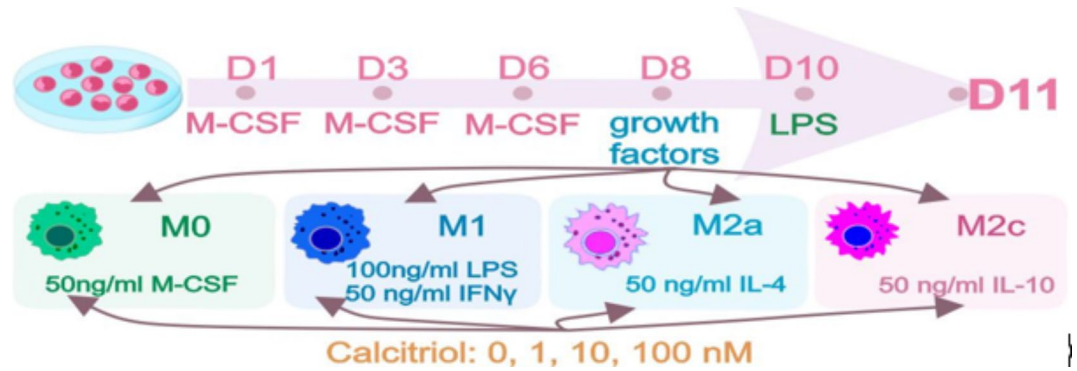
Fig. 1. Scheme of the differentiation of monocytes from the peripheral blood of patients into macrophage (MDM) classes. The cells were differentiated in the presence of M-CSF from the day of culture initiation to day 7, and the media were replaced with fresh media on days 3 and 6. On the eighth day, the MDMs were treated with factors differentiating them into macrophage classes: M0 (initial cells, stimulating factor: M-CSF 50 ng/mL), M1 (stimulating factor: LPS 100 ng/mL, INFγ 50 ng/mL), M2a (stimulatory factor: IL-4 50 ng/mL) and M2c (stimulatory factor: IL-10 50 ng/mL). The differentiation process was carried out in the absence or presence of calcitriol (1, 10, and 100 nM). After 48 h, the cells were treated with LPS for another 24 h. On day 11, the cells were collected for phenotypic analysis (flow cytometry). M-CSF, macrophage colony stimulating factor: 50 ng/mL; LPS, lipopolysaccharide: 100 ng/mL; INFγ, interferon gamma: 50 ng/mL; IL-4, interleukin 4:50 ng/mL; IL-10, interleukin 10:50 ng/mL.

Name	Clone/producer	Surface marker
CD11b-FITC	ICRF44/BioLegend	Myeloid cells
CD14-BV-421	M5E2/BioLegend	Monocytes/macrophages
CD200R-APC	OX-108/BioLegend	M2a
(HLA-DR) MHC II PerCP/Cy5.5	Tü36/BioLegend	M1
CD163-PE	GHI/61/BioLegend	M2c
CD204-BV650	U23-56/BD Biosciences	M2a
CD80-BV785	2D10/BioLegend	M1
CD44-BV510	IM7/BioLegend	M2
CD45-FITC	HI30/BioLegend	Leukocyte common antigen

Table 3. List of antibodies used for cytometric analysis.

Aldrich, Saint-Louis, MO, USA), 0.1 mg/mL streptomycin and 100 U/mL penicillin (Polfa Tarchomin, Warsaw, Poland)) and mechanically disassembled using a scalpel. The precrushed material was transferred to a 10 mL test tube, supplemented to a volume of 4 mL with medium containing 1 mg/mL collagenase IV (collagenase from *Clostridium histolyticum*; Sigma-Aldrich, Saint-Louis, MO, USA) and DNAse I (Roche, Basel, Switzerland), and incubated at 37 °C for 2 h with gentle shaking. The homogenate was then filtered through a 70 μm cell strainer into a sterile 50 mL test tube and topped to a volume of 20 mL with PBS solution containing 1% FBS. The cell suspension was centrifuged (10 min, 300×g, 4 °C), and after suspension in 5 mL of separation buffer, cell viability was counted and assessed. The next steps were similar for materials from blood and tumors. For each of the further stages of isolation, a buffer consisting of PBS (pH 7.2), 0.5% BSA (bovine serum albumin), and 2 mM EDTA (Sigma-Aldrich, Saint-Louis, MO, USA).

For each further isolation stage, antiCD14 antibodies combined with magnetic beads (Miltenyi Biotec, Auburn, CA, USA) were used for separation. In the case of tumor material, receptors for Fc fragments of antibodies were blocked for 5 min using antiCD16/CD32 antibodies (TruStain FcX BioLegend, San Diego, CA, USA, catalog number #422302). The cells were then incubated with antibodies for 30 min at 4 °C, followed by magnetic separation using MS magnetic columns (Miltenyi Biotec, Auburn, CA, USA) according to the manufacturer's instructions. The isolated cells were then subjected to further manipulations.

Preparation of protein lysates and measurement of protein levels
Protein lysates were prepared using RIPA buffer supplemented with a cocktail of phosphatase 2 and 3 inhibitors and protease inhibitors (1/100 μL of buffer; Sigma-Aldrich, Saint Louis, MO, USA). Tumor tissues preserved in liquid nitrogen and stored at −80 °C were thawed, weighed, and transferred to homogenized ampoules containing ceramic beads and an appropriate amount of RIPA buffer supplemented with protease and phosphatase inhibitors (500 μL for every 300 mg of tissue). The samples were homogenized in a FastPrep device (MP Biomedicals LLC, Santa Ana, CA, USA) using the parameters CY 24×2, 5.5 m/s, and $t = 40$ s, with the cycle repeated twice. The lysates were then frozen in liquid nitrogen and stored at −80 °C.

On the day of western blot analysis preparation, the samples were thawed on ice, centrifuged at 10,000×g at 4 °C for 10 min, and the supernatants were transferred to new tubes. The protein concentration was determined using the modified Lowry method (DC Protein Assay Bio-Rad, Hercules, CA, USA)[35,36]. A BSA standard curve (2–0.125 mg/mL; Bio-Rad, Hercules, CA, USA) was used to determine the protein concentration in the samples, with absorbance measurements performed using a Synergy H4 Hybrid Multi-Mode Microplate Reader (BioTek Instruments, Inc., Winooski, VT, USA).

Western blot

Samples containing the appropriate amount of protein were prepared in 4× Laemmli Sample Buffer (Bio-Rad Laboratories, Hercules, CA, USA) containing β-mercaptoethanol (βME) (Merck, Darmstadt, Germany). A volume containing 50 μg of protein was placed on the gel track after the mixture was boiled at 98 °C. Polyacrylamide gels of various densities were used for electrophoretic separation (SDS-PAGE), depending on the size (kDa) of the proteins being determined. The PageRuler Plus Prestained Protein Ladder mass marker (#26616; Thermo Fisher Scientific, Waltham, MA, USA) was used as a control for determining the size of the proteins being detected.

Electrophoretic separation was carried out using parameters of 100 V (constant parameter), 0.6 A, and 300 W for approximately 1 h and 20 min. The next step was the semidry transfer of the separated proteins from the gel onto a PVDF membrane (6×9 cm) (Immobilon-FL, Merck KGaA, Darmstadt, Germany) on blotting paper (Bio-Rad, Hercules, CA, USA) soaked in a buffer containing glycine (7.2 g), Trizma base (1.51 g), and methanol (100 mL; Polish Chemical Reagents, Gliwice, Poland) dissolved in 500 mL of Milli-Q water. This process took an hour at 0.3 A (constant parameter) and 25 V. After transfer, the membrane was blocked for an hour using a solution of skim milk dissolved in TBS with 0.1% Tween-20 (TBST). Then, after a series of 4 washes (4×5 min), the membrane was incubated overnight at 4 °C with an antibody solution prepared at the appropriate concentration (listed in Table 4) in TBST with 5% blocking solution. The next day, the membranes were incubated for an additional 30 min at room temperature with the primary antibody. After another series of washes (TBST; 4×5 min), the following secondary antibodies were applied: mouse antirabbit IgG-HRP (1:10,000) (sc-2357; Santa Cruz Biotechnology, Dallas, TX, USA) or goat antimouse IgG-HRP (1:2000) (P0447; Dako, Carpinteria, CA, USA), depending on the I-layer antibody used. After the incubation, the membranes were washed again (with TBST; 4×5 min), and the proteins were detected using Clarity Western ECL Substrate reagent (Bio-Rad, Hercules, CA, USA). Chemiluminescence was visualized using a ChemiDoc Imaging System (Bio-Rad, Hercules, CA, USA). Densitometric analysis was performed using ImageJ 1.48r (National Institutes of Health, Bethesda, MA, USA) by comparing the band intensity of the studied proteins to that of β-actin, which served as a loading control.

Analysis of cell surface markers by flow cytometry

Cytometric analysis was conducted on TAMs freshly isolated from tumors upon receiving the patients' postoperative tissue. MDMs were analyzed on the final day of the ex vivo experiments. For analysis, cells were collected in PBS supplemented with 2% FBS and centrifuged at 324×g at 4 °C for 5 min. In the case of MDMs, the cell suspension was blocked using antiCD16/CD32 antibodies (5 min; room temperature, 0.1 μg/100 μL; TruStain FcX BioLegend, San Diego, CA, USA, catalog number #422302), while (blocked before the process separation), the TAM cell suspension in PBS was stained for 30 min at 4 °C using the eBioscience Fixable Viability Dye eFluor 780 dye (0.1/100 μL; Invitrogen, Waltham, MA, USA), enabling the separation of dead and living cells in the analysis. After washing away the blocking solution or dye (by centrifugation at 324×g at 4 °C), the cells were suspended in a solution containing the antibody mixture (Table 3). The cells were incubated for 30 min at 4 °C. Subsequently, the samples were sequentially washed in 2% FBS in PBS, suspended in 200 μL of PBS, and analyzed using a BD LSRFortessa flow cytometer (BD Biosciences, San Jose, CA, USA). The results were analyzed using the BD FACS Diva 6.2 program, and the fluorescence intensity was determined relative to that of the unstained control (MFI).

Protein	Clone/catalog number	Dilution*
EpCAM, epithelial cell adhesion molecule antigen	21050-1-AP	1:1000
OPN, osteopontin	22952-1-AP	
ZEB-1, proteins from the E-Box zinc finger family binding Homeobox 1	21544-1-AP	1:1000
VDR, vitamin D receptor	D2K6W/#12,550	
CYP24A1, 24-hydroxylase	H-87/#sc-66,851	
CYP27B1, 1α-hydroxylase	EPR20271/ab206655	
MMP-3, metalloproteinase 3	JM46-22/NBP2-75931	
IRF4, interferon regulatory factor 4	11247-2-AP	1:500
TGFβ, transforming growth factor β	21898-1-AP	
S100A8, S100 calcium-binding protein A8	15792-1-AP	1:1000
PTHLH, parathyroid hormone-like hormone	NBP3-03168	
Vimentin	NBP1-31327	1:5000

Table 4. Rabbit monoclonal and polyclonal antibodies used for protein immunodetection. *The antibodies were diluted in TBST solution supplemented with blocking solution (10:1).

Statistical analysis

Statistical analysis of the results was conducted using the GraphPad Prism 7.01 software (https://www.graphpad.com, GraphPad Software Inc., USA) for data analysis and visualization. The normality of the data distribution was checked using the Shapiro−Wilk test. An ANOVA was performed for data with a Gaussian distribution, while data deviating from the Gaussian distribution were analyzed using the Kruskal−Wallis test. Correlation analysis was conducted using the nonparametric Spearman correlation. Details of each test are provided in the figure or table legends, and statistically significant differences were considered when $P < 0.05$.

Results

Expression of selected proteins in tumor tissue and surface markers in TAMs isolated from tumors

Cancer tissue from 80 patients was characterized in terms of the expression of key proteins related to the mechanism of action of VD, the metastasis process, and the importance of macrophage function. The expression of various proteins (ratio of protein tested/β-actin) including VDR, CYP24A1, CYP27B1, OPN, S100A8, PTHLH, MMP3, vimentin, EpCAM, IRF4, TGFβ, and ZEB-1, was analyzed (Fig. 2, Additional file 1: Table S1).

EpCAM expression in tumors was significantly lower in VD-deficient patients compared to VD-normal patients ($P < 0.05$) (Fig. 2A). Although not statistically significant ($P = 0.0545$), increased expression of CYP24A1 was detected in VD-deficient and HER2⁻ patients. IRF4 expression was higher in premenopausal patients than in postmenopausal patients ($P = 0.0583$). When comparing protein expression between nonmetastatic and LN-metastatic patients, there was a tendency toward increased expression of OPN ($P = 0.053$) and decreased expression of PTHLH ($P = 0.095$) in nonmetastatic patients (Additional file 1: Table S1).

Patients were also divided according to the level of CYP27B1 in tumor tissue (based on its median value) (Table 1). The expression of TGFβ, EpCAM, and OPN was significantly higher in tumors with high CYP27B1 expression (Fig. 2B), while the expression of IRF4 was significantly lower (Fig. 2C). There was a tendency toward higher expression of MMP3 ($P = 0.0581$) and lower expression of CYP24A1 ($P = 0.0750$) with high expression of CYP27B1. VDR, vimentin, ZEB1, and PTHLH expression did not differ significantly in this respect (Additional file 1: Figure S2).

TAMs were isolated from tumor tissues collected from 54 patients. The isolated cells were assessed for the expression of molecules characteristic of different macrophage classes, including CD11b, CD14, CD80, HLA-DR, CD163, CD200R, and CD44 (Additional file 1: Table S2). The only differences observed between the individual patient groups were significantly lower numbers of TAMs expressing HLA-DR and CD44 in nonmetastatic patients compared to those with metastases to regional lymph nodes (LN-metastatic) (Fig. 2F). TAMs isolated from tumors with high CYP27B1 expression exhibited significantly lower expression of CD200R, CD204, and CD44. The expression of the other analyzed molecules did not significantly differ (Fig. 2G). The gating strategy for flow cytometry analyses is shown as an example of CD11b staining (Fig. 2H).

Uncropped western blot images for all analyzes presented in this work are included in Supplementary information 2.

Additional file 1: Figure S2 shows representative histograms of the data presented in Fig. 2F and G and noncropped blots of the data presented in Fig. 2D and E.

Furthermore, we calculated correlations between factors important for VD, namely, plasma levels of VD (a 25(OH)D₃ metabolite), VDR, CYP24A1, and CYP27B1, and the above-described tumor tissue and TAM characteristics. All statistically significant correlations observed (in any patient group) are summarized in Additional file 1: Table S3–S5. Additional File 1 Table S6 summarized hormone and HER2 receptors correlations with VD related parameters (plasma levels of VD, VDR, CYP24A1, and CYP27B1). However, only correlations close to 0.5 and greater were taken into account in further considerations and are presented here.
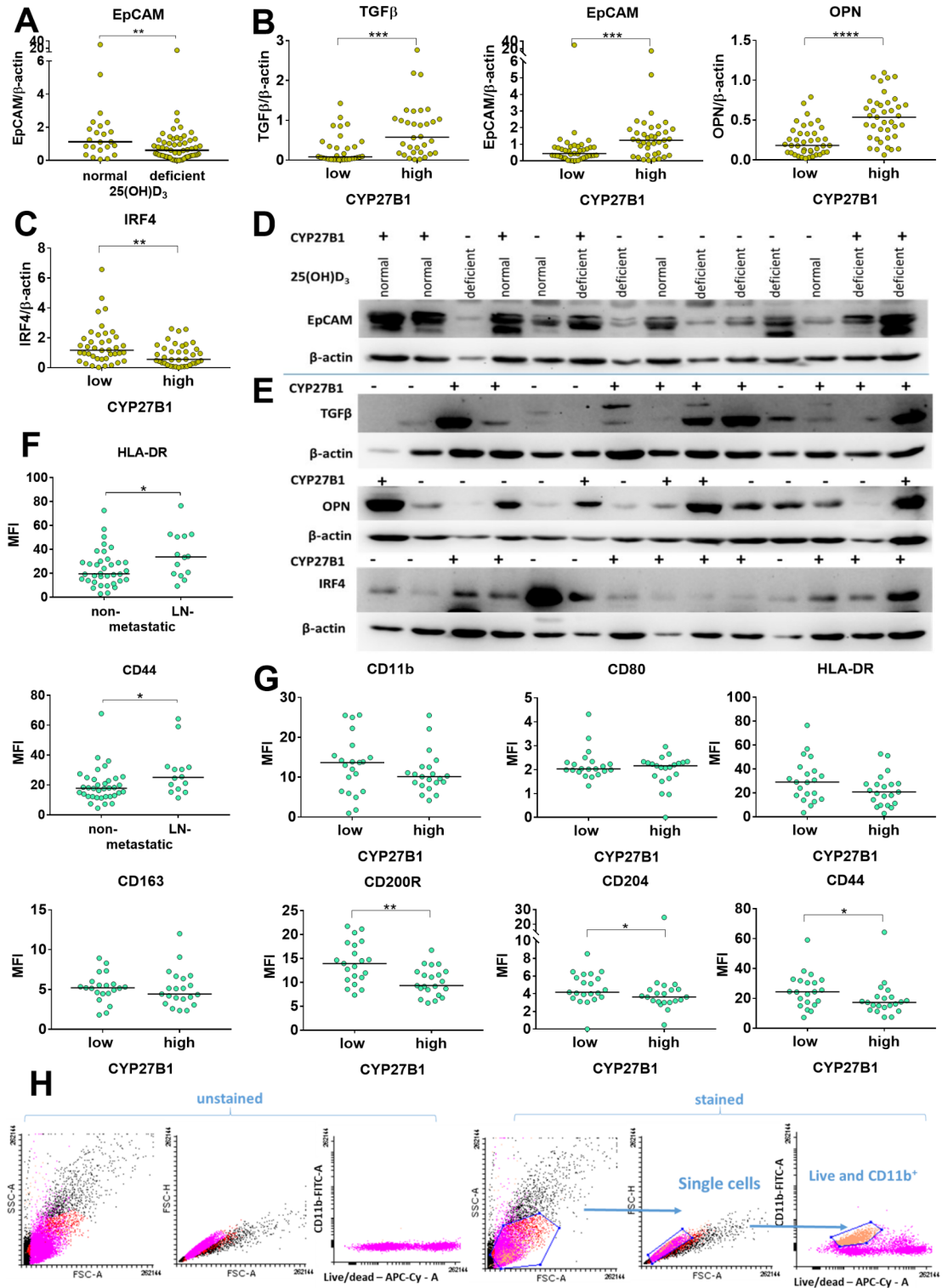
Tumor tissue correlations

The plasma concentration of 25(OH)D₃ (ng/mL) was positively correlated with IRF4 and ZEB1 expression (protein tested/β-actin ratio) in tumor tissue from patients with normal VD levels. In premenopausal patients, it was positively correlated with IRF4 expression. Conversely, a negative correlation was found between the plasma 25(OH)D₃ concentration and the CYP24A1 concentration in tumor tissue from patients with LN metastases (Fig. 3A). VDR expression was positively correlated with ZEB1 in VD-normal and premenopausal patients and with CYP24A1 in VD-deficient and LN-metastatic patients (Fig. 3B). CYP24A1 was negatively correlated with EpCAM in postmenopausal and LN-metastatic patients and with OPN in LN-metastatic patients (Fig. 3C).

A positive correlation between CYP27B1 and TGFβ was detected in the whole group of patients, as well as in patients with normal VD levels, premenopausal and postmenopausal patients, and nonmetastatic and LN-metastatic patients (Fig. 4A). CYPP27B1 was also positively correlated with OPN in all patients, as well as in each patient subgroup (Fig. 4B). In postmenopausal patients, CYP27B1 inversely correlated with IRF4 (Fig. 4C), and in nonmetastatic and LN-metastatic patients, CYP27B1 was positively correlated with EpCAM (Fig. 4D).

Positive correlations of OPN with TGFβ were detected in all patients, as well as in the VD-normal and VD-deficient subgroups, and the postmenopausal and nonmetastatic subgroups (Fig. 5A). In patients with normal VD levels, OPN expression was positively correlated with EpCAM expression (Fig. 5B). This correlation between OPN positivity and EpCAM expression was also observed in postmenopausal and LN-metastatic patients (Fig. 5B). Supplementary Table S7 summarizes the OPN correlations in all groups of patients.

TAM correlations

The plasma level of 25(OH)D₃ was positively correlated with CD80 expression on TAMs isolated from tumor tissue of patients with normal 25(OH)D₃ levels (Fig. 6A). CYP27B1 expression was negatively correlated with CD200R expression in all, VD-deficient, premenopausal, and nonmetastatic patients (Fig. 6B). In patients with

normal 25(OH)D$_3$ levels, CD80 expression correlated negatively with CYP27B1 expression in tumor tissue (Fig. 6C). There was also a negative correlation between CYP27B1 and CD204 and CD44 in postmenopausal and nonmetastatic patients and between CYP27B1 and HLA-DR in premenopausal and nonmetastatic patients (Fig. 6D–F, respectively). The correlations for the remaining groups of patients are presented in Additional file 1: Table S8.

Impact of calcitriol on MDM differentiation

Compared with M0 MDM, control monocytes from all patients (not treated with calcitriol) that differentiated into particular classes of macrophages were characterized by increased (M1 and M2c) or decreased (M2a) CD14 expression, decreased (M1) or increased (M2a) CD11b expression, increased expression of CD80 (M1), increased expression of CD200R (M1 and M2a), and increased expression of CD163 (M2c) (Additional file

◀ **Fig. 2**. Tumor tissue and TAM characteristics—selected protein expression. (**A**) EpCAM expression in tumor tissue from patients with various 25(OH)D$_3$ plasma levels. $N = 23$ normal; $N = 57$ deficient. (**B**) Tumor tissue expression of transforming growth factor β (TGFβ; $N = 32$), epithelial cell adhesion molecule antigen (EpCAM; $N = 39–40$), osteopontin (OPN; $N = 39–40$) and (**C**) IRF4 ($N = 38–40$) in patients with low and high CYP27B1 (1α-hydroxylase) expression in tumor tissue. (**A-C**) Proteins expression was analyzed by western blot and protein tested/β-actin ratio is provided. (**D**) Representative blots showing EpCAM expression. (**E**) Representative blots showing TGFβ, OPN, and IRF4 expression. The patients were described as (**D**) for plasma 25(OH)D$_3$ concentration (normal or deficient) and (**D**) and (**E**) for CYP27B1 expression (high + and low −). TAMs expression of (**F**) HLA-DR and CD44 isolated from metastatic and nonmetastatic patients ($N = 14–36$) and of **G** CD11b, CD80, HLA-DR, CD163, CD200R, CD204, and CD44 in patients with low and high CYP27B1 expression in tumor tissue ($N = 21$) were evaluated. (**H**) Gating strategy for flow cytometry analyses; CD11b staining is shown as an example. (**F-H**) The data were visualized using Flowing Software version 2.5.1. (https://flowingsoftware.com) and the fluorescence intensity was determined relative to that of the unstained control (MFI). Statistical analysis: Mann–Whitney test; *$P < 0.05$, **$P < 0.01$, ***$P < 0.001$, ****$P < 0.0001$.
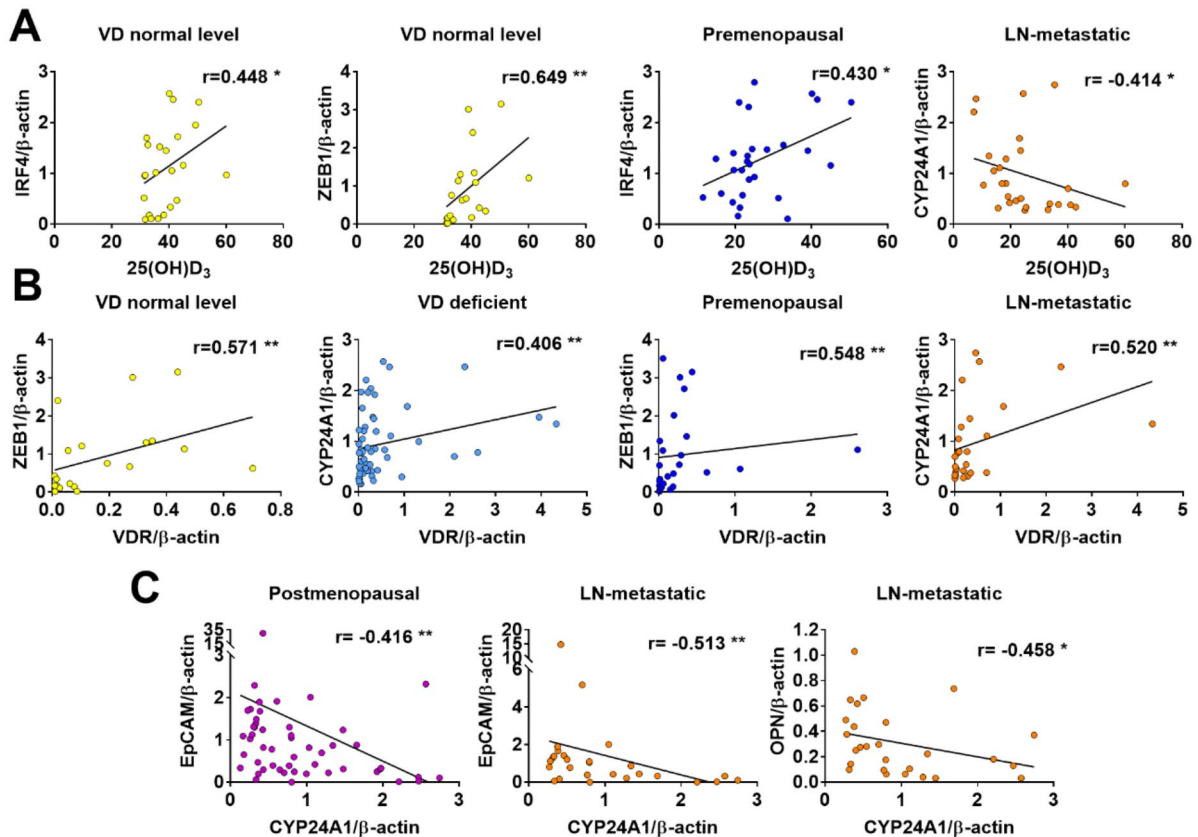
Fig. 3. Correlations of vitamin D$_3$ (VD)-related factors with the expression of selected proteins in tumor tissue. Spearman correlation coefficients for (**A**) 25(OH)D$_3$ [ng/mL], (**B**) VDR, and (**C**) CYP24A1. The numbers of patients were as follows: (**A**) VD-normal IRF4, $N = 23$; ZEB1, $N = 20$; premenopausal, IRF4, $N = 28$; lymph node metastatic (LN-metastatic), CYP24A1, $N = 27$; (**B**) VD-normal, ZEB1, $N = 20$; VD-deficient, CYP24A1, $N = 57$; premenopausal, ZEB1, $N = 26$; LN-metastatic, CYP24A1, $N = 27$; and (**C**) postmenopausal, EpCAM, $N = 51$; and LN-metastatic, EpCAM and OPN, $N = 27$. IRF4, interferon-regulatory factor 4; ZEB1, proteins from the E-Box zinc finger family binding homeobox 1; CYP24A1, 24-hydroxylase; VDR, vitamin D receptor; EpCAM, epithelial cell adhesion molecule antigen; OPN, osteopontin; *$P < 0.05$, **$P < 0.01$.

1: Figure S3). To assess the effect of calcitriol on such differentiated cells, they were exposed to calcitriol at concentrations of 1, 10, and 100 nM. Statistical analyses were performed for all patients from whom monocytes were isolated and divided into subgroups. The results were analyzed using the BD FACS Diva™ 6.2 program, and the fluorescence intensity was determined relative to that of the unstained control (MFI). The gating strategy for flow cytometry analyses and representative histograms are presented in Additional file 1: Figure S4.
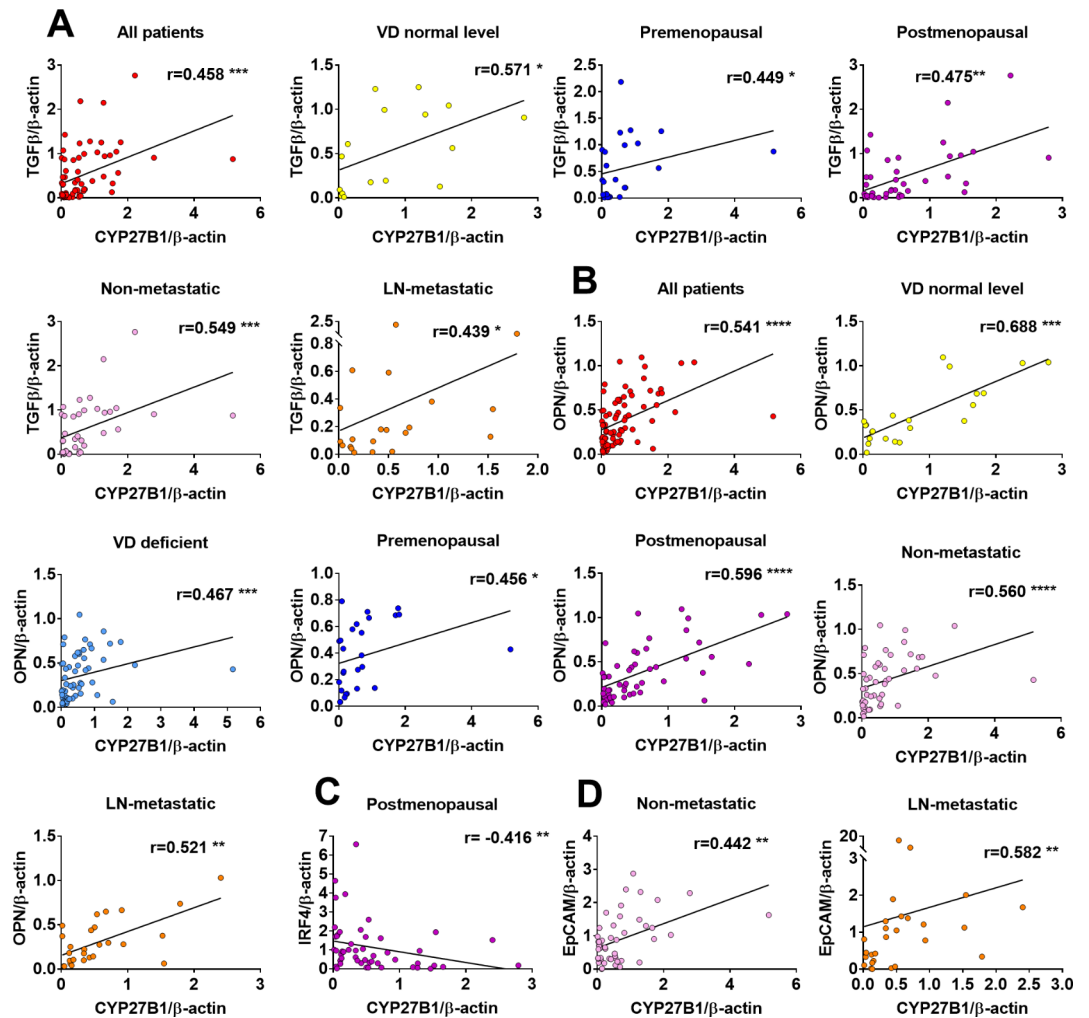
Fig. 4. CYP27B1 correlations with tumor tissue proteins. Spearman r correlations of CYP27B1 with (**A**) TGFβ: all patients $N=64$, VD-normal $N=16$, premenopausal $N=24$, postmenopausal $N=40$, nonmetastatic $N=39$, LN-metastatic $N=21$; (**B**) OPN: all patients $N=79$, VD-normal $N=22$, VD-deficient $N=57$, premenopausal $N=28$, postmenopausal $N=51$, nonmetastatic $N=48$, LN-metastatic $N=27$; (**C**) IRF4: postmenopausal $N=40$; (**D**) EpCAM: nonmetastatic $N=48$, LN-metastatic $N=27$. TGFβ, transforming growth factor β; OPN, osteopontin; IRF4, interferon-regulatory factor 4; EpCAM, epithelial cell adhesion molecule antigen; CYP27B1, 1α-hydroxylase; VD, vitamin D_3; *$P<0.05$, **$P<0.01$, ***$P<0.001$, ****$P<0.0001$.

All patients

The expression of CD11b, CD200R, CD204, and CD44 was not affected by calcitriol during macrophage differentiation (Additional file 1: Figure S5). Calcitriol increased CD14 expression in M0 (100 nM) and M1 (10 and 100 nM) macrophages (Fig. 7A). Similarly, calcitriol decreased HLA-DR expression in M0, M1, M2a, and M2c macrophages (10 and 100 nM) (Fig. 7B). Calcitriol decreased CD80 expression in M0 (10 nM) and M2c (1–100 nM) macrophages (Fig. 7C). The level of CD163 was decreased by calcitriol in M0 (10 nM) and M2c (10 nM) macrophages (Fig. 7D).

Patients with normal VD levels

The expression of CD11b, CD80, CD204, CD44, and CD163 was not affected by calcitriol during macrophage differentiation in patients with a normal level of 25(OH)D$_3$ (Additional file 1: Figure S6). Calcitriol increased CD14 expression in M0 (100 nM), M1 (100 nM), and M2c (100 nM) macrophages. The level of HLA-DR was decreased by calcitriol only in M0 (10 nM) and M1 (100 nM) macrophages. Additionally, CD200R expression was decreased by 100 nM calcitriol in M1 macrophages (Fig. 8A–C).

Patients with VD deficiency

The expression of CD11b, CD200R, CD204, and CD44 was not affected by calcitriol during macrophage differentiation in patients with VD deficiency (Additional file 1: Figure S7). Calcitriol increased CD14 expression in M0 (100 nM) and M1 (10 and 100 nM) macrophages. The level of HLA-DR was decreased by calcitriol in M0, M1, M2a (10 and 100 nM), and M2c (100 nM) macrophages. Calcitriol decreased CD80 expression in M0 (10
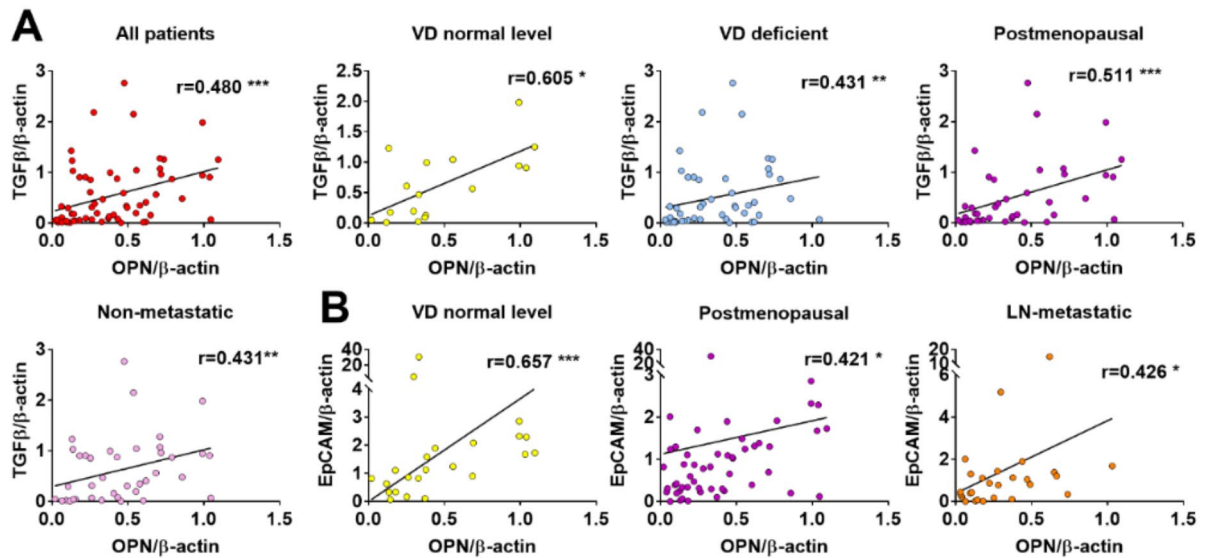
Fig. 5. Correlations of OPN with other tumor tissue proteins. Spearman r correlations of OPN with (**A**) TGFβ: all patients, $N = 65$; VD-normal, $N = 17$; VD-deficient, $N = 48$; postmenopausal, $N = 41$; nonmetastatic, $N = 40$; (**B**) EpCAM: VD-normal, $N = 23$; postmenopausal, $N = 52$; and LN-metastatic, $N = 27$. TGFβ, transforming growth factor β; EpCAM, epithelial cell adhesion molecule antigen; OPN, osteopontin; VD, vitamin D$_3$; $*P < 0.05$, $**P < 0.01$, $***P < 0.001$.

nM) and M2c (10 and 100 nM) macrophages. The level of CD163 was decreased by calcitriol in M0 (10 nM) and M2c (10 nM) macrophages (Fig. 8D–G).

Premenopausal patients
In premenopausal patients, CD11b, CD200R, CD204, CD44, and CD163 were not significantly affected by calcitriol during macrophage differentiation (Additional file 1: Figure S8). Calcitriol increased CD14 expression in M0 (100 nM) and M1 (10 nM) macrophages. The level of HLA-DR was decreased by calcitriol in M0 (10 nM), M1, and M2a (100 nM) macrophages. Calcitriol decreased CD80 in M1 (100 nM) macrophages (Fig. 9A–C).

Postmenopausal patients
The expression of CD11b, CD200R, CD204, and CD44 was not affected by calcitriol during macrophage differentiation in postmenopausal patients (Additional file 1: Figure S9). Calcitriol increased CD14 expression in M0 (100 nM) and M1 (10 and 100 nM) macrophages. The level of HLA-DR was decreased by calcitriol in M0, M1, M2a (10 and 100 nM), and M2c (100 nM) macrophages. Calcitriol decreased CD80 expression in M0 (10 nM) and M2c (10 and 100 nM) macrophages. Moreover, calcitriol decreased CD163 expression in M2c (10 nM) macrophages (Fig. 9D–G).

Nonmetastatic patients (N0M0)
In nonmetastatic patients, CD11b, CD200R, CD204, and CD44 were not affected by calcitriol during macrophage differentiation (Additional file 1: Figure S10). Calcitriol increased CD14 expression in M0 (100 nM) and M1 (10 and 100 nM) macrophages. The level of HLA-DR was decreased by calcitriol in M0, M1, M2a (10 and 100 nM), and M2c (100 nM) macrophages. Calcitriol decreased CD80 in M0 and M2c (10 nM) macrophages. The level of CD163 was decreased by calcitriol in M2c (10 nM) macrophages (Fig. 10A–D).

Patients with LN metastases (N + M0)
In patients with metastases in sentinel LNs, CD11b, CD80, CD200R, CD204, CD163, and CD44 were not affected by calcitriol during macrophage differentiation (Additional file 1: Figure S11). Calcitriol increased CD14 expression in M0 and M1 (100 nM) macrophages. The level of HLA-DR was decreased by calcitriol only in M0 (100 nM) macrophages (Fig. 10E, F).

Patients with distant metastases (M1)
In patients with distant metastases, CD11b, CD80, CD204, and CD44 were not affected by calcitriol during macrophage differentiation (Additional file 1: Figure S12). Calcitriol increased CD14 expression in M1 and M2a (100 nM) macrophages. The level of HLA-DR was decreased by calcitriol in M2c (10 and 100 nM) macrophages. Calcitriol decreased CD163 in M0 (100 nM) and M2c (10 nM) macrophages (Fig. 10G–I). Example histograms illustrating the CD163 expression on M0 and M2c MDMs from patients with distant metastases are shown in Fig. 10J.
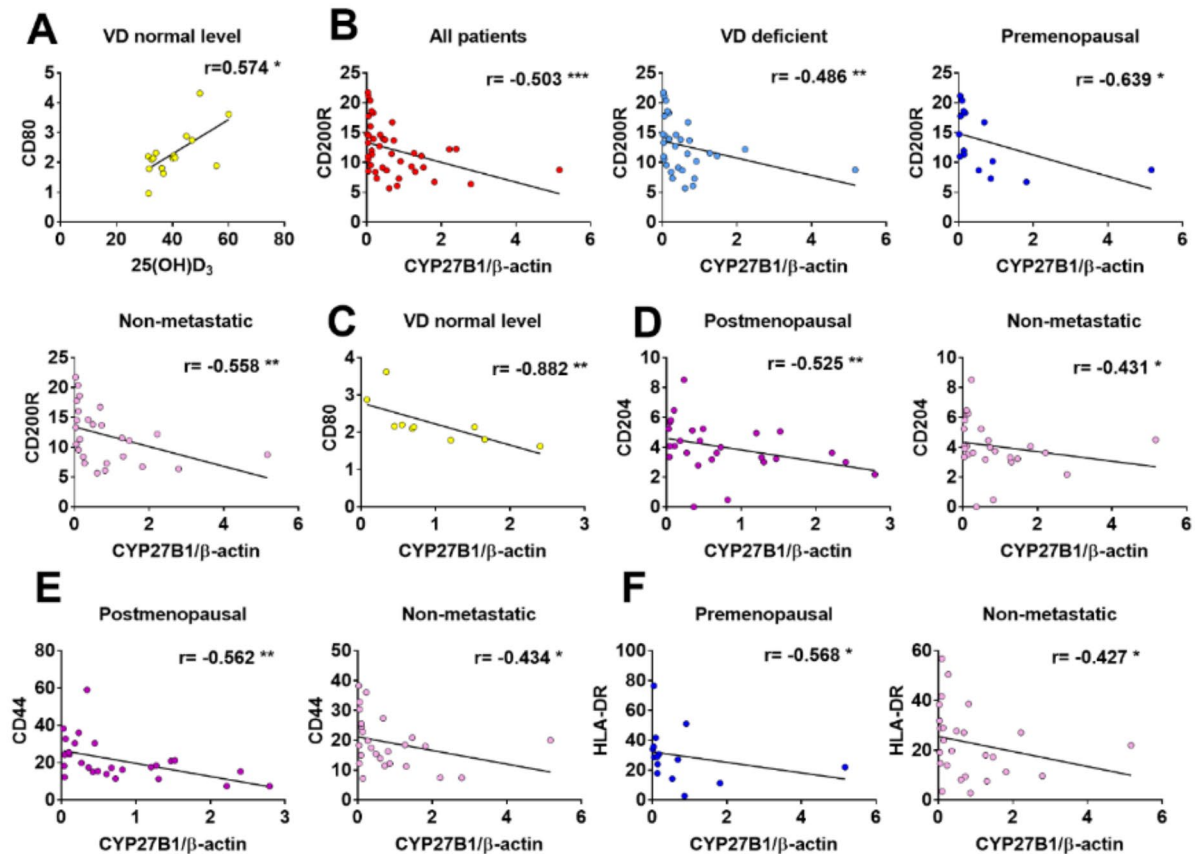
Fig. 6. Correlations of TAMs with the plasma concentration of 25(OH)D$_3$ and the expression of CYP27B1 in tumor tissue. (**A**) Spearman r correlations of 25(OH)D$_3$ [ng/mL] with CD80; $N = 16$. Spearman r correlations of 25(OH)D$_3$ with (**B**) CD200R (all patients: $N = 42$, VD-deficient: $N = 31$, premenopausal: $N = 15$, nonmetastatic: $N = 26$), (**C**) CD80 ($N = 16$), (**D**) CD204 (postmenopausal: $N = 27$, nonmetastatic: $N = 26$), (**E**) CD44 (postmenopausal: $N = 27$, nonmetastatic: $N = 26$), and F HLA-DR (premenopausal: $N = 15$, nonmetastatic: $N = 26$). CYP27B1, 1α-hydroxylase; VD, vitamin D$_3$; The expression of TAMs markers were analyzed using the BD FACS Diva™ 6.2 program, and the fluorescence intensity was determined relative to that of the unstained control (MFI). The expression of CYP27B1 was analyzed by western blot and CYP27B1/β-actin ratio are determined. $*P < 0.05$, $**P < 0.01$, $***P < 0.001$.

Monocyte correlations
The expression of control monocyte (nontreated) markers was correlated with the plasma 25(OH)D$_3$ concentration (Additional file 1: Table S10, Fig. 11). The plasma concentration of 25(OH)D$_3$ negatively correlated with CD80 expression on M2a and M2c macrophages (from patients with a normal level of VD and premenopausal patients, respectively), as well as with CD163 on M0 macrophages from LN-metastatic patients (Fig. 11).

Discussion

Many studies have been conducted on the effect of VD on macrophages, primarily using cell lines or cells from mice. These studies generally suggest that VD polarizes macrophages toward the M2 phenotype[29,37], although other reports indicate the opposite effect[38]. In our studies using a 4T1 mouse model of breast cancer, we found that calcitriol-stimulated M2 polarization of macrophages might result from the activation of COX-2 and prostaglandin E2 (PGE2) synthesis in cancer cells[33]. Other authors have shown that the VD analog paricalcitol reduced M2 polarization in a xenograft mouse model of breast cancer by promoting the intracellular degradation of β-catenin[39]. However, we could not find any studies in the literature where cells from breast cancer patients were analyzed in this way.

Zhang et al. demonstrated a negative correlation between VDR expression and metastasis in breast cancer patients. They also showed that overexpression of VDR in breast cancer cells alleviated the prometastatic effect and induced epithelial-to-mesenchymal transition (EMT) when cocultured with macrophage cell line. Additionally, they found that calcitriol administration had antimetastatic effects on breast cancer cells both in vitro and in vivo in a mouse model of breast cancer by preserving VDR and suppressing β-catenin[40]. In our studies, the expression of VDR, CYP24A1, and CYP27B1 did not significantly differ between LN-metastatic and nonmetastatic patients or between other groups of patients. VDR expression also did not correlate with any
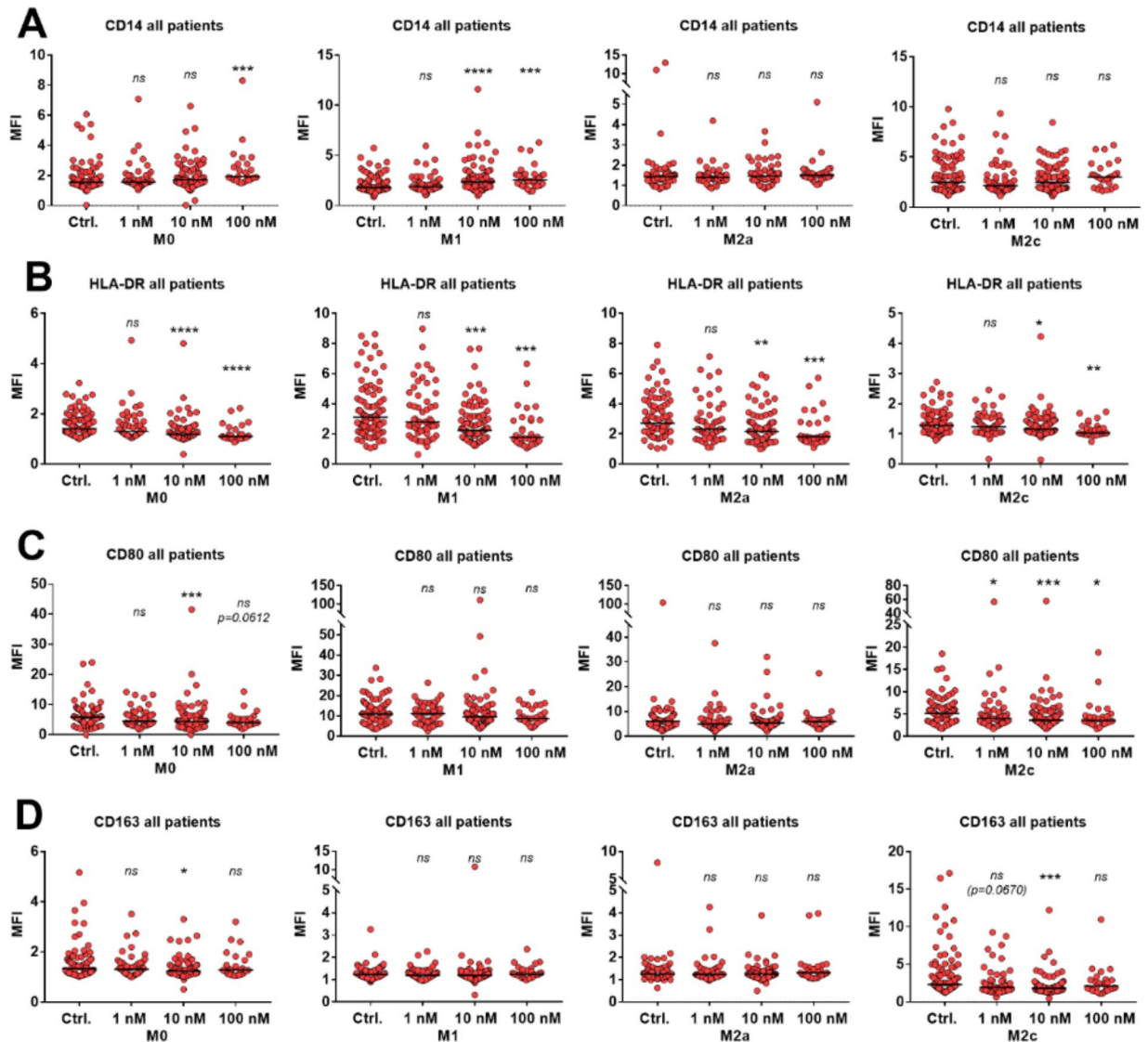
Fig. 7. Impact of calcitriol on the differentiation of MDMs from breast cancer patients (all). Expression of (**A**) CD14, (**B**) HLA-DR, (**C**) CD80, and (**D**) CD163 on M0, M1, M2a, and M2c macrophages. The cells were differentiated in the presence of M-CSF for 7 days, and the medium was replaced with fresh medium on days 3 and 6. On the eighth day, the MDMs were treated with factors differentiating them into macrophage classes: M0 (initial cells, stimulating factor: M-CSF 50 ng/mL), M1 (stimulating factor: LPS 100 ng/mL, INFγ 50 ng/mL), M2a (stimulatory factor: IL-4 50 ng/mL) and M2c (stimulatory factor: IL-10 50 ng/mL). The differentiation process was carried out in the absence or presence of calcitriol (1, 10, and 100 nM). After 48 h, the cells were treated with LPS for another 24 h. On day 11, the cells were collected for phenotypic analysis (flow cytometry analysis using the BD FACS Diva™ 6.2 program, and the fluorescence intensity was determined relative to that of the unstained control, MFI). M-CSF, macrophage colony stimulating factor; LPS, lipopolysaccharide; INFγ, interferon gamma; IL-4, interleukin 4; IL-10, interleukin 10. Additional file 1: Table S9 presents the detailed numbers of patients in each group analyzed. Statistical analysis: Dunn's multiple comparison test; *ns*, nonsignificant; $*P < 0.05$, $**P < 0.01$, $***P < 0.001$, $****P < 0.0001$.

TAM markers. In our previous studies with the same patient groups, we also found no correlation between VDR and CAF activation, density, or infiltration[34]. However, VDR expression in tumor tissue positively correlated with CYP24A1 in VD-deficient and LN-metastatic patients, a finding not observed in previous studies[41]. Cells positive for VDR can respond to calcitriol, which can upregulate CYP24A1. The CYP24A1 enzyme inactivates calcitriol by hydroxylating the 24-carbon, resulting in the formation of 1,24,25-trihydroxyvitamin D_3[14]. We also showed that tumoral CYP24A1 is inversely correlated with CAF density and infiltration, suggesting an inhibitory effect of calcitriol on CAFs[34]. CAFs, TAMs, and tumor cells have dynamic and reciprocal relationships
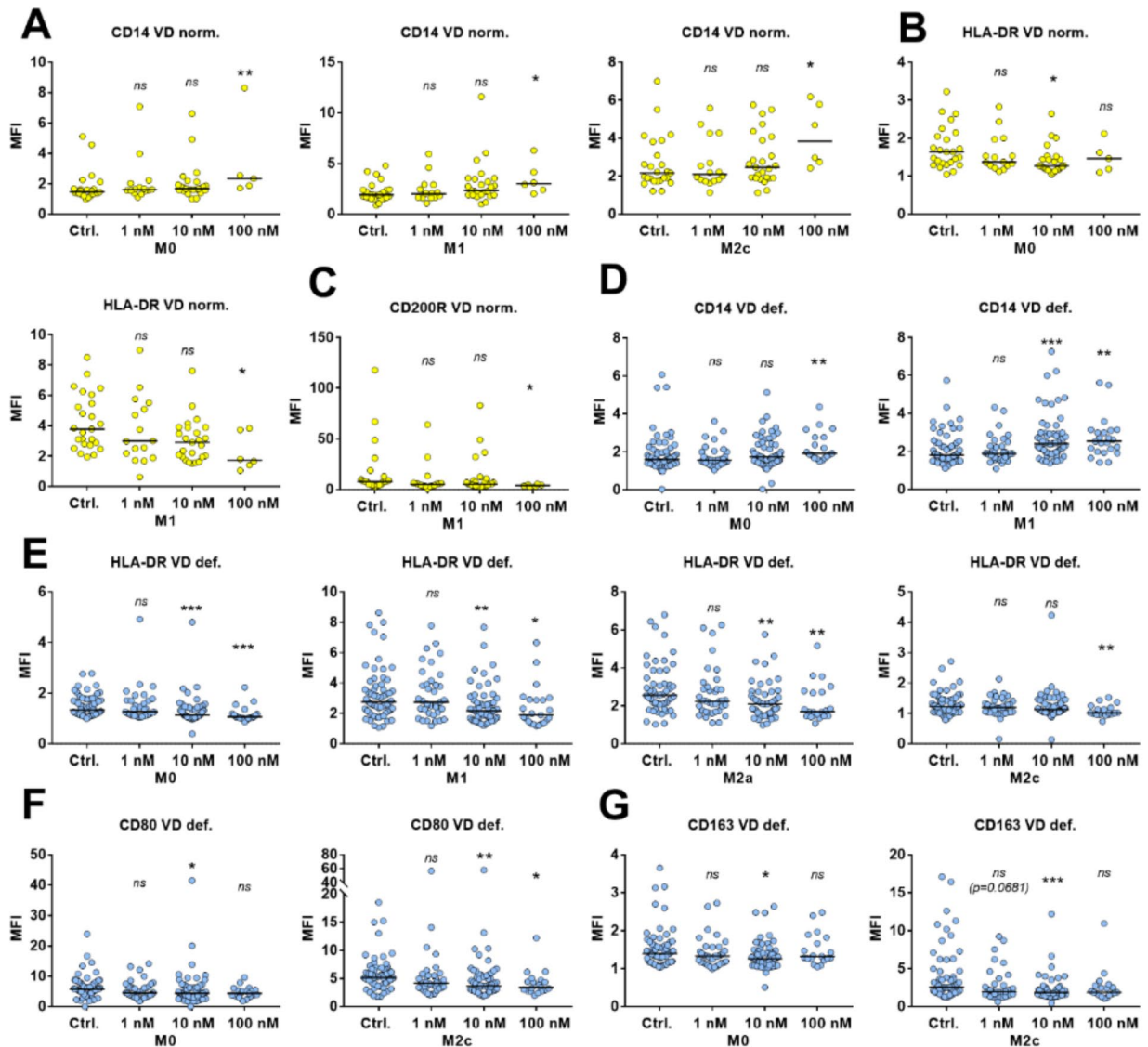
Fig. 8. Impact of calcitriol on the differentiation of MDMs from breast cancer patients (VD-normal and VD-deficient). (**A**) CD14, (**B**) HLA-DR, and (**C**) CD200R expression in MDMs from breast cancer patients with normal $25(OH)D_3$ plasma concentrations. Expression of (**D**) CD14, (**E**) HLA-DR, (**F**) CD80 and (**G**) CD163 on MDMs from VD-deficient patients. The cells were differentiated in the presence of M-CSF for 7 days, and the medium was replaced with fresh medium on days 3 and 6. On the eighth day, the MDMs were treated with factors differentiating them into macrophage classes: M0 (initial cells, stimulating factor: M-CSF 50 ng/mL), M1 (stimulating factor: LPS 100 ng/mL, INFγ 50 ng/mL), M2a (stimulatory factor: IL-4 50 ng/mL) and M2c (stimulatory factor: IL-10 50 ng/mL). The differentiation process was carried out in the absence or presence of calcitriol (1, 10, and 100 nM). After 48 h, the cells were treated with LPS for another 24 h. On day 11, the cells were collected for phenotypic analysis (flow cytometry analysis using the BD FACS Diva™ 6.2 program, and the fluorescence intensity was determined relative to that of the unstained control, MFI). M-CSF, macrophage colony stimulating factor; LPS, lipopolysaccharide; INFγ, interferon gamma; IL-4, interleukin 4; IL-10, interleukin 10. Additional file 1: Table S9 presents the detailed numbers of patients in each group analyzed. Statistical analysis: Dunn's multiple comparison test; *ns*, nonsignificant; $*P < 0.05$, $**P < 0.01$, $***P < 0.001$.

with each other[42], and VD, which can affect each of these cell subpopulations differently, can modulate the TME in an anticancer direction.

CYP27B1, responsible for converting $25(OH)D_3$ to calcitriol, is found in tumor tissue, including breast cancer cells[14,23]. The level of CYP27B1 in tumor tissue, which may indicate the level of calcitriol in the TME[23] correlates with many TAM markers. TAMs are identified mainly by the M2 class of macrophages and have procancer properties. Characteristic features of this group of macrophages include low surface levels of HLA-
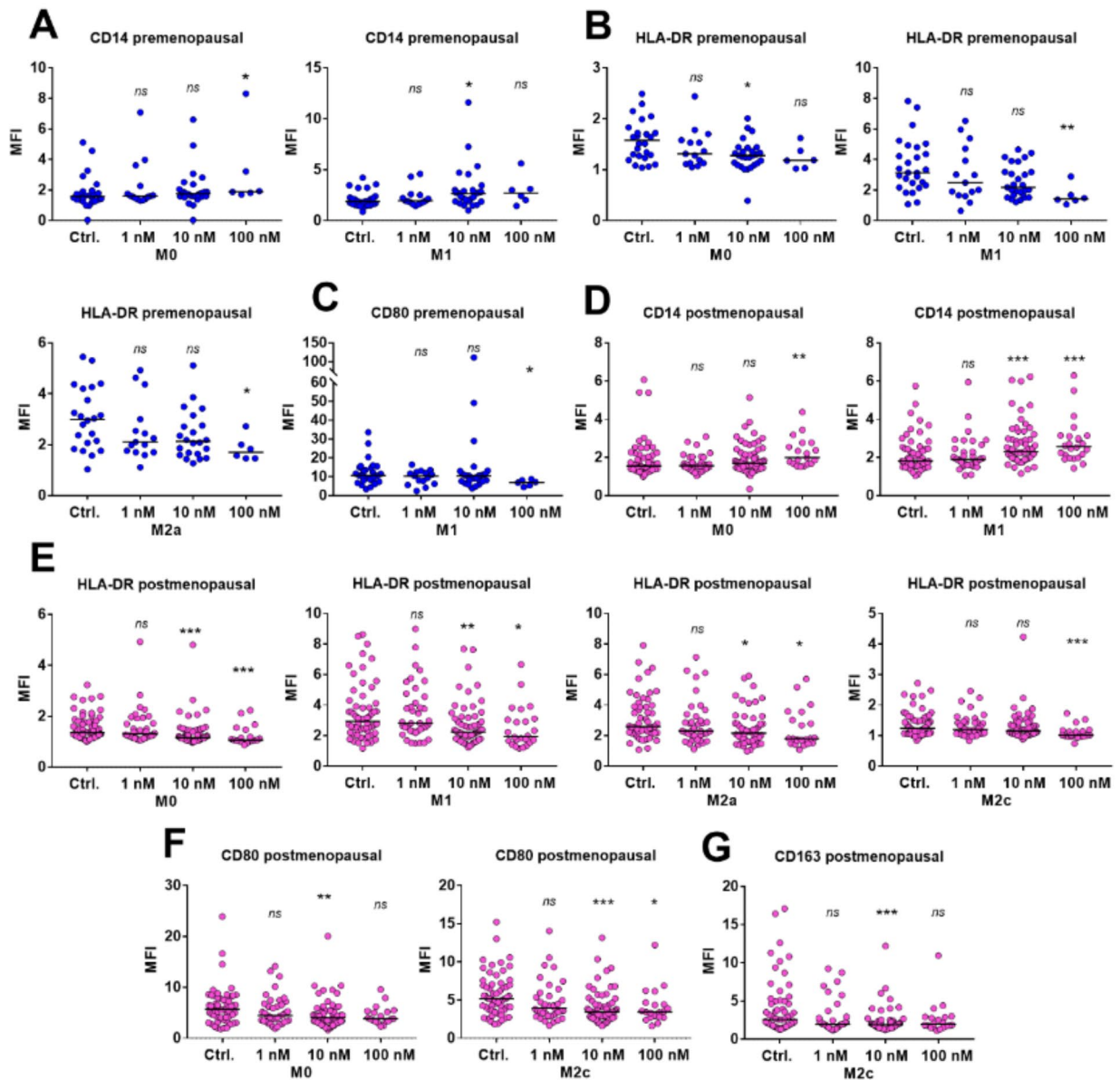
Fig. 9. Impact of calcitriol on the differentiation of MDMs from breast cancer patients (premenopausal and postmenopausal). (**A**) CD14, (**B**) HLA-DR, and (**C**) CD80 expression in MDMs from premenopausal breast cancer patients. Expression of (**D**) CD14, (**E**) HLA-DR, (**F**) CD80, and (**G**) CD163 on MDMs from postmenopausal patients. The cells were differentiated in the presence of M-CSF for 7 days, and the medium was replaced with fresh medium on days 3 and 6. On the eighth day, the MDMs were treated with factors differentiating them into macrophage classes: M0 (initial cells, stimulating factor: M-CSF 50 ng/mL), M1 (stimulating factor: LPS 100 ng/mL, INFγ 50 ng/mL), M2a (stimulatory factor: IL-4 50 ng/mL) and M2c (stimulatory factor: IL-10 50 ng/mL). The differentiation process was carried out in the absence or presence of calcitriol (1, 10, and 100 nM). After 48 h, the cells were treated with LPS for another 24 h. On day 11, the cells were collected for phenotypic analysis (flow cytometry analysis using the BD FACS Diva™ 6.2 program, and the fluorescence intensity was determined relative to that of the unstained control, MFI). M-CSF, macrophage colony stimulating factor; LPS, lipopolysaccharide; INFγ, interferon gamma; IL-4, interleukin 4; IL-10, interleukin 10. Additional file 1: Table S9 presents the detailed numbers of patients in each group analyzed. Statistical analysis: Dunn's multiple comparison test; *ns*, nonsignificant; *$P < 0.05$, **$P < 0.01$, ***$P < 0.001$.
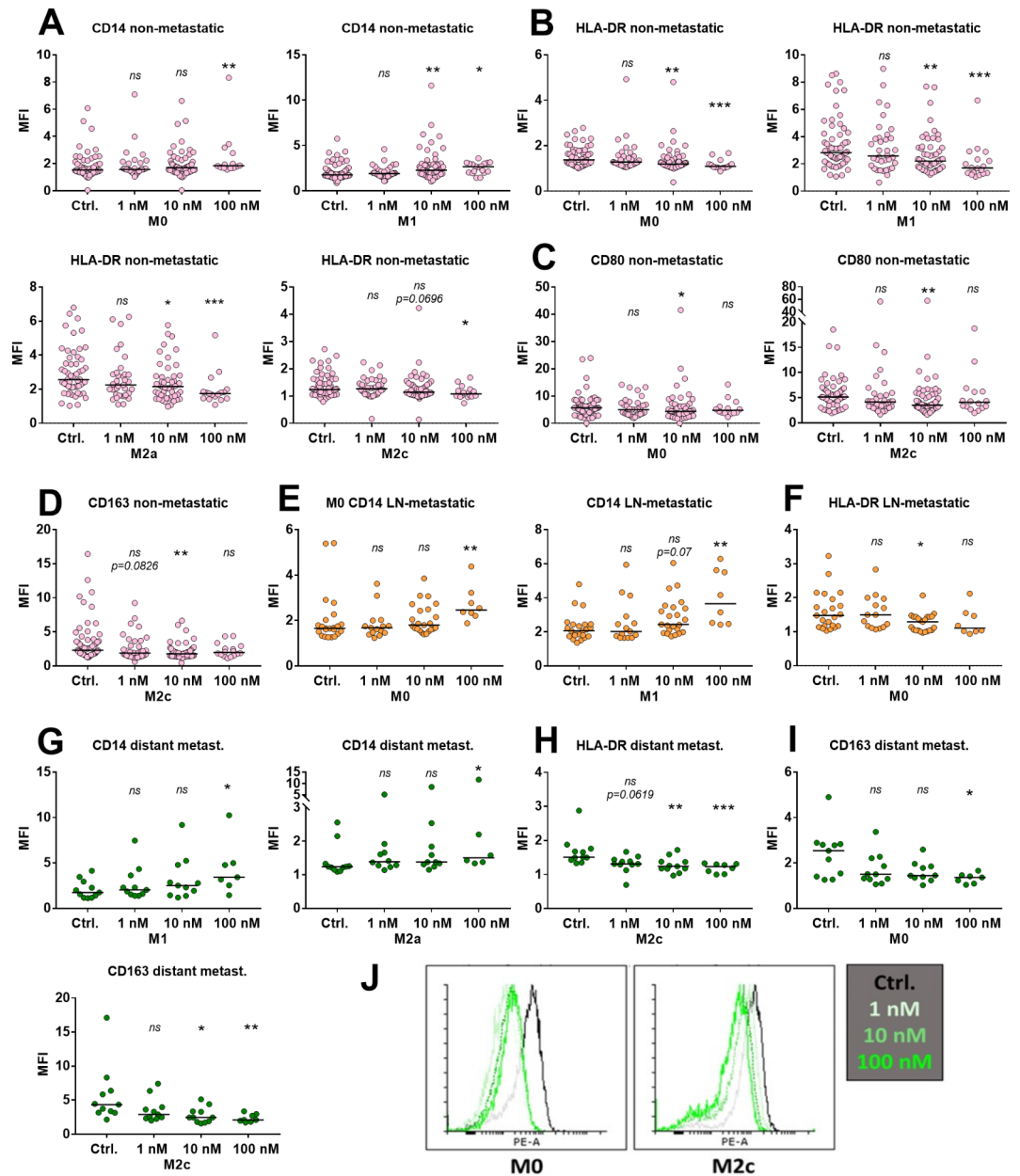
Fig. 10. Impact of calcitriol on the differentiation of MDMs from breast cancer patients (nonmetastatic, LN-metastatic and with distant metastases). Expression of (**A**) CD14, (**B**) HLA-DR, (**C**) CD80, and (**D**) CD163 in MDMs from nonmetastatic breast cancer patients. Expression of (**E**) CD14 and **F** HLA-DR on MDMs from LN-metastatic patients. Expression of (**G**) CD14, (**H**) HLA-DR, and (**I**) CD163 on MDMs from patients with distant metastases. (**J**) Example histograms illustrating the data presented in Graph I (CD163 expression on M0 and M2c MDMs from patients with distant metastases). Monocytes were differentiated in the presence of M-CSF for 7 days, and the medium was replaced with fresh medium on days 3 and 6. On the eighth day, the MDMs were treated with factors differentiating them into macrophage classes: M0 (initial cells, stimulating factor: M-CSF 50 ng/mL), M1 (stimulating factor: LPS 100 ng/mL, INFγ 50 ng/mL), M2a (stimulatory factor: IL-4 50 ng/mL), and M2c (stimulatory factor: IL-10 50 ng/mL). The differentiation process was carried out in the absence or presence of calcitriol (1, 10, and 100 nM). After 48 h, the cells were treated with LPS for another 24 h. On day 11, the cells were collected for phenotypic analysis (flow cytometry analysis using the BD FACS Diva™ 6.2 program, and the fluorescence intensity was determined relative to that of the unstained control, MFI). M-CSF - macrophage colony stimulating factor; LPS, lipopolysaccharide; INFγ, interferon gamma; IL-4, interleukin 4; IL-10, interleukin 10; LN, lymph nodes. Additional file 1: Table S9 presents the detailed numbers of patients in each group analyzed. Statistical analysis: Dunn's multiple comparison test; *ns*, nonsignificant; *$P < 0.05$, **$P < 0.01$, ***$P < 0.001$.
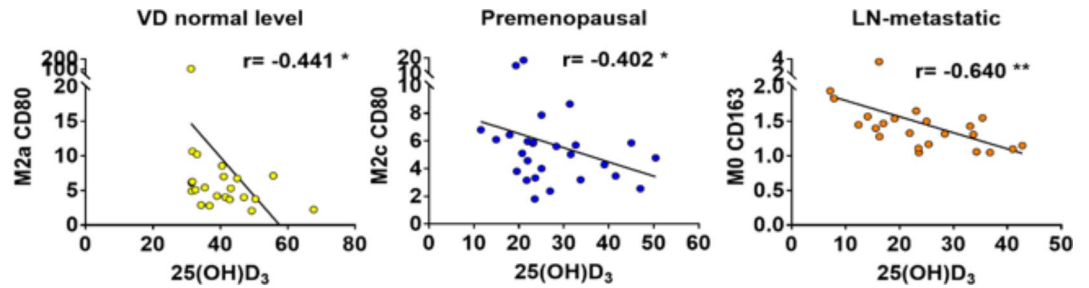
Fig. 11. Correlations of the plasma 25(OH)D$_3$ concentration with macrophage markers on MDMs differentiated into various classes. Spearman r correlations of 25(OH)D$_3$ with CD80 on M2a ($N = 23$) and M2c ($N = 27$) and with CD163 on M0 ($N = 23$) MDMs. *$P < 0.05$, **$P < 0.01$.

DR, high levels of markers such as CD206, CD204, and CD163, and increased levels of arginase 1 (Arg-1)[43]. They secrete anti-inflammatory cytokines like IL-10 and TGFβ[44] and often release factors supporting angiogenesis or molecules related to the transformation of the extracellular matrix (ECM), such as vascular endothelial growth factor (VEGF), TGFβ, epidermal growth factor (EGF), and metalloproteinase 9 (MMP-9)[45]. Mantovani et al. further classified M2-type macrophages into subgroups: M2a, M2b, M2c, and M2d. M2a, activated by IL-4, promotes fibrosis and Th2 response; M2b, activated by TLR or IL-1R agonists, has immunoregulatory functions and induces Th2 response; M2c, activated by IL-10, is associated with immunosuppression, tissue repair, and ECM reorganization; and M2d, activated by IL-6, is considered to neovascularization and metastasis induction[46]. In our studies, TAM expression of CD200R, characteristic of M2a macrophages[47], negatively correlated with CYP27B1 in all patient groups, including VD-deficient, premenopausal, and nonmetastatic patients. Furthermore, patients with high CYP27B1 expression had significantly lower CD200R TAM levels. High-dose calcitriol decreased ex vivo CD200R expression on M1 MDMs in patients with normal VD concentrations. CD204 TAM expression, also associated with M2 macrophages, negatively correlated with CYP27B1 in postmenopausal and nonmetastatic patients, and was lower in patients with high CYP27B1 expression. CD204-positive macrophages have been linked to worse prognosis in breast cancer patients[48]. CD44, another marker of M2 macrophages[49], inversely correlated with CYP27B1 in postmenopausal and nonmetastatic patients and was lower in patients with high CYP27B1 expression. However, these findings did not translate to ex vivo studies where calcitriol did not affect CD200R, CD204, or CD44 expression in monocytes isolated from breast cancer patients and differentiated into macrophages (with the exception of M1 CD200R inhibition by 100 nM calcitriol).

The immunophenotype of M1 macrophages typically includes surface markers such as HLA-DR, CD80, and CD86. These cells predominantly secrete proinflammatory cytokines like IL-12, IL-1, IL-6, IL-23, and interferons. Despite their well-documented antitumor functions, M1 macrophages may paradoxically contribute to tumor growth. Nitric oxide and reactive oxygen species produced by M1 macrophages can induce genetic instability in cells, while high levels of IL-6 and tumor necrosis factor (TNFα) promote cancer cell proliferation and angiogenesis[50–52].

In our studies, we observed negative correlations between CD80 and HLA-DR TAM expression and CYP27B1 levels in VD-normal (CD80) and premenopausal or nonmetastatic (HLA-DR) patients. Additionally, in patients with normal VD levels and premenopausal patients, CD80 expression in M2a and M2c macrophages (respectively; control, nontreated ex vivo with calcitriol) was negatively correlated with plasma 25(OH)D$_3$ concentration. Moreover, during MDM differentiation across all patient groups, calcitriol reduced HLA-DR expression, while CD80 was also significantly decreased except for patients with normal VD levels or those with LN and distant metastases (Fig. 12).

The observations related to VD from this study, such as the decrease in M1 and M2 macrophage markers by calcitriol or their negative correlation with CYP27B1, suggest a modulatory, anticancer activity of VD in the tumor microenvironment (TME). However, the extent of these effects varied among patient groups (Fig. 12). The most notable effects of calcitriol on the breast cancer microenvironment were observed in patients without metastases (N0M0). In these patients, as well as in postmenopausal, VD-deficient, and patients with distant metastases, calcitriol reduced the expression of CD163, particularly on MDMs differentiated ex vivo toward M2c. CD163 is often used as a molecular characteristic of M2-type macrophages[47,53]. What is more, in the literature, there is often described an association between CD163$^+$ macrophages infiltration and its correlation with worse clinical characteristics of patients and, as in the case of CD68$^+$ macrophages, it depends on the tumor subtype—mainly triple-negative and HER-2$^+$ cancers[53–56].

In all patient groups, calcitriol induced CD14 expression. The calcitriol-induced increase in myeloid cell differentiation with increased CD14 expression is a well-known phenomenon[57–59]. However, the induction of CD14 expression varied among patient groups. Patients with normal VD levels showed an increase in CD14 expression on M0 and M1 MDMs, as well as on M2c. Increased CD14 expression on M2 (M2a) macrophages was also observed in patients with distant metastases. Furthermore, compared to patients with normal VD levels, M1-class MDMs from VD-deficient patients were more sensitive to differentiation, showing increased CD14 expression after treatment with 10 nM calcitriol. Similar increases in CD14 expression in M1 macrophages after treatment with 10 nM calcitriol were observed in premenopausal and postmenopausal patients and patients with node metastases. Therefore, MDMs from patients without metastases, postmenopausal patients,
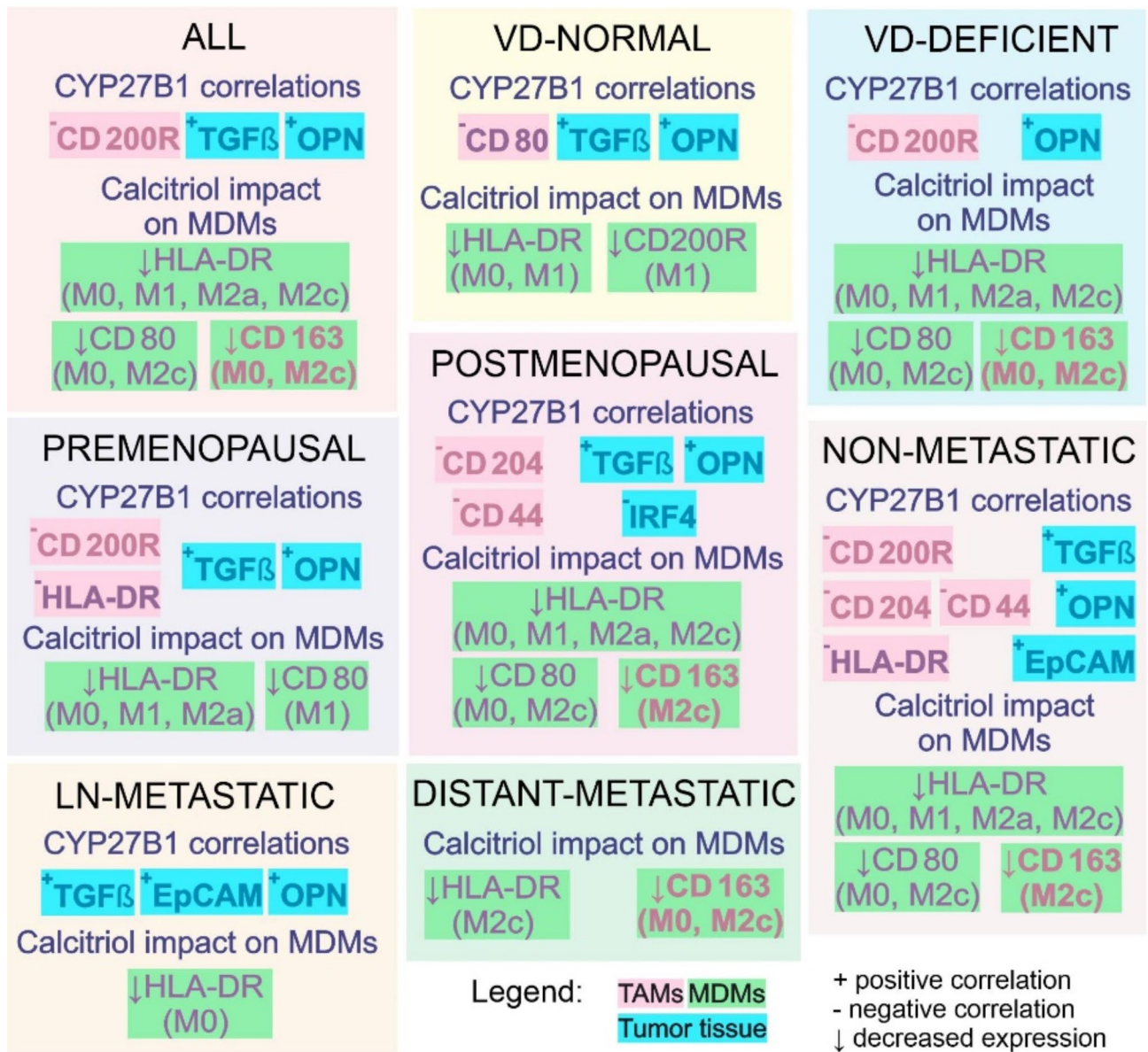
Fig. 12. VD decreased M1 and M2 macrophage markers. Summary of the most frequently observed correlations in tumor tissue and the ex vivo effect of calcitriol on the differentiation of MDMs into different classes.

and VD-deficient patients appear to be the most sensitive to the influence of calcitriol ex vivo. Among them, postmenopausal patients and patients without metastases exhibit the greatest effects of calcitriol on TAMs and protein expression in the tumor, as correlated with CYP27B1 expression. Conversely, patients with normal VD concentrations and patients with node metastases (the most important results are summarized in Fig. 12).

To clarify the differences between the ex vivo effect of calcitriol on MDM differentiation and the observed correlations in tumor tissue between CYP27B1 expression and TAM characteristics, we analyzed the expression of selected factors in tumor tissue that could have influenced these results. We found that tumors with high CYP27B1 expression also exhibited significantly increased expression of TGFβ, except in VD-deficient patients. The induction of TGFβ by calcitriol has been described in human breast cancer cell culture[60] although conflicting results have also been reported[61]. In our studies using a 4T1 murine mammary carcinoma model transplanted into young or aged ovariectomized mice (representing premenopausal and postmenopausal models), we observed increased (in young) or decreased (in aged) levels of *Tgfb1* in the lungs of these mice (the main site of metastasis of this tumor)[30,62]. However, in the same mice, calcitriol and its analogs reduced TGFβ levels in tumor tissue and increased plasma TGFβ concentrations in young mice[31] without affecting them in aged mice[30]. The duplicitous effect of calcitriol described in the literature with its effect on TGFβ is further complicated by knowledge about the effect of TGFβ on macrophage populations and the tumor microenvironment. TGFβ is a

pleiotropic cytokine that, on the one hand, may have an antitumor effect on less advanced or a prometastatic effect on more advanced tumors, and it can stimulate M2 polarization[63,64].

We also observed higher levels of OPN in tumors with higher CYP27B1 expression across all patient groups. OPN expression is regulated by VD at the genomic level[65], so the high OPN expression in these tumors may be a direct result of this mechanism. In addition to its many unfavorable effects, such as promoting metastasis and angiogenesis, OPN in the TME is responsible for maintaining the M2 phenotype of macrophages[66]. CD44 is one of the receptors for OPN[67], and we observed lower TAM expression of CD44 in patients with high OPN expression (and high CYP27B1 expression). A calcitriol derivative was previously shown to repress CD44 expression in human breast cancer MCF10DCIS.com cells both in vitro and in xenograft tumors[68]. Therefore, the effect of calcitriol on the tumor microenvironment may be twofold, and the predominance of one of these processes may determine the final effect in individual patients.

Positive correlations between TGFβ and OPN with CYP27B1 were observed in all patient groups (except for VD deficiency and TGFβ expression). In the case of EpCAM, this correlation was detected only in certain groups (nonmetastatic and LN metastatic), with higher expression of this protein also detected in tumors with higher CYP27B1 expression. Moreover, in postmenopausal patients, EpCAM expression was negatively correlated with CYP24A1 expression. EpCAM overexpression is strongly correlated with poor survival and prognosis in most types of cancer, such as ovarian and breast cancers, and helps identify patients at high risk of recurrence (e.g., in prostate cancer)[69–72]. Besides being a characteristic marker for epithelial cells, its role as a biomarker of cancer stem cells and circulating tumor cells is well recognized[69,73]. However, the roles of EpCAM in cancer progression are highly context-dependent and can even be contradictory[74]. In a mouse model of cholestatic liver disease, the calcitriol analog paricalcitol increased EpCAM expression[75]. However, in 4T1 mouse mammary gland tumor tissue, a high cholecalciferol diet significantly decreased EpCAM expression, while calcitriol administered to mice fed a VD-deficient diet increased EpCAM expression[33]. In addition, we observed positive correlations of EpCAM (and TGFβ) with OPN. Therefore, intersecting (including contradictory) direct and indirect effects of VD on the tumor microenvironment cannot be ruled out and require further research.

The differences between patients with normal VD levels and those with VD deficiency suggest less favorable effects of calcitriol on TAMs or MDMs in patients with normal VD levels. This could be due to a lower degradation of calcitriol in these patients, possibly resulting from a tendency toward lower expression of CYP24A1 in tumors ($P = 0.0545$). Additionally, higher expression of EpCAM was observed in the tumors of patients with normal VD levels. Previous studies also indicated higher expression of β-catenin and TGFβ in the tumors of these patients compared to those with VD deficiency[34]. These phenomena may explain why only TAM CD80 expression was negatively correlated with CYP27B1 in patients with normal VD levels.

A comparison between premenopausal and postmenopausal patients revealed that calcitriol potentially weakened the polarization of TAMs toward the M2 phenotype in postmenopausal patients but had a smaller effect in premenopausal patients. Additionally, a decrease in CD163 on the M2c phenotype was confirmed only in postmenopausal patients. Moreover, a negative correlation between IRF4 and CYP27B1 was observed in postmenopausal patients, with low IRF4 expression also observed in patients with high CYP27B1 expression. Nevertheless, in patients with normal VD levels and premenopausal patients, IRF4 was positively correlated with plasma 25(OH)D$_3$. IRF4 promotes the M2 polarization of macrophages in the TME[76]. The available literature on the regulation of IRF4 expression by calcitriol shows different results, depending on the experimental model. For example, in inflammatory bowel disease, calcitriol polarizes macrophages toward the M2 phenotype and simultaneously increases IRF4 expression[77]. However, during the differentiation of human monocytes into dendritic cells, calcitriol blocks the induction of IRF4[78]. In our studies, bone marrow-derived macrophages harvested from young mice bearing 4T1 tumors and treated with calcitriol displayed elevated *Irf4* gene expression, and these tumors were also more prone to metastasis[33]. IRF4 expression was lower in postmenopausal patients than in premenopausal patients ($P = 0.0583$), possibly due to the direct effect of estrogens on the regulation of the expression of this molecule[79,80]. In studies on animals bearing 4T1 mouse mammary gland cancer, we showed that calcitriol may have different effects on macrophages depending on the age of the mouse. In young mice treated with calcitriol, we observed an increased percentage of Ly6C^{low} splenocytes, which are capable of differentiating toward M2[81], and a reduction in their percentage in aged mice subjected to ovariectomy (postmenopausal model)[30]. Additionally, the Th2 immune response predominates in young mice with 4T1 tumors treated with VD[62]. In addition to animal studies, epidemiological studies also indicate that premenopausal and postmenopausal patients may differ in their response to VD supplementation or its plasma level. A meta-analysis including prospective studies of circulating VD (dose−response) and breast cancer risk suggested a differential breast cancer risk by menopause, with a gradual inverse association observed in postmenopausal women above the 27 ng/mL threshold but with a flattening of effects above 35 ng/mL of 25(OH)D[82]. Another study showed an association between high VD serum levels and self-reported VD supplementation and a decreased risk of breast cancer, which was particularly strong among postmenopausal women[83].

TAMs and MDMs from patients with cancer metastasizing to regional lymph nodes appear to be resistant to VD, especially compared to patients without metastases. However, in patients with distant metastases, ex vivo calcitriol reduced the expression of CD163 on M0 and M2c MDMs. The mechanism by which calcitriol inhibits M2c differentiation observed by decrease in CD163 expression may be associated with the STAT3 signaling pathway. Notably, the action of IL-10 relies on activating STAT3, whereas recently, the impact of calcitriol on inhibiting STAT3 has been demonstrated in renal cell carcinoma[84]. What is more, it was revealed that calcitriol blocks pSTAT3 nuclear translocation as a result of increased VDR/pSTAT3 interaction in PC-3 and DU-145 prostate cancer cell lines[85]. This could indirectly explain the observed effect. Animal studies using murine mammary carcinomas with different metastatic capacities also showed differences in the effect of calcitriol on TAMs. For the most invasive mouse mammary gland cancer, 4T1, increased polarization of TAMs toward the M2 phenotype was observed. In the case of the less invasive but also metastatic cancer E0771, these effects

were less severe and indicated a decrease in M2 polarization, although, in E0771 mice with VD deficiency, CD163 expression was increased in vivo by calcitriol. A similar effect of CD163 on TAMs was observed in the case of nonmetastatic 67NR tumors (without affecting other markers)[33]. Although these effects observed in mouse models do not correlate with individual groups of patients, a strong differentiation of effects can also be observed, depending mainly on the characteristics of cancer cells. For example, 4T1 cells treated with calcitriol in vitro are characterized by an increase in COX-2 expression, while 67NR is characterized by a decrease in COX-2 expression, and E0771 does not respond significantly to such treatment[33]. Another example is the difference in tumor expression of OPN (4T1 > E0771 > 67NR) or TGFβ (4T1 = E0771 > 67NR) between these mouse mammary gland cancers[86]. Some clinical studies also show stronger antitumor effects of VD observed in patients with no detectable circulating tumor cells (CTCs). Namely, CTC-negative patients, with VD levels above the median, have been found to have better survival compared to patients with detected CTCs[87]. However, further studies are needed to explain these differences in the effects of VD on cancer cells with different metastatic potential.

Conclusions

In conclusion, calcitriol, or VD in general, has various effects on macrophages themselves and on the tumor microenvironment, with the intensity of these effects depending on the group of patients examined. Based on these studies, it can be argued that the most pronounced calcitriol-dependent effects are observed in N0M0 and postmenopausal patients. Despite the potentially unfavorable VD effects on TGFβ, OPN, or EpCAM expression in tumors from these patients, the effect on TAMs and MDMs is generally beneficial. The lowest potential anticancer effect of calcitriol was observed in N1M0 patients. However, the observational nature of conducted studies and the use of semi-quantitative methods in assessing individual markers necessitate further analyses to verify the discussed relationships and their clinical applicability.

Data availability

All data generated or analyzed during this study are included in this published article and its supplementary information files.

References

1. Vanhevel, J., Verlinden, L., Doms, S., Wildiers, H. & Verstuyf, A. The role of Vitamin D in Breast cancer risk and progression. *Endocrine-Relat. Cancer.* https://doi.org/10.1530/ERC-21-0182 (2022).
2. Filip-Psurska, B., Zachary, H., Strzykalska, A., Wietrzyk, J. & Vitamin, D. Th17 lymphocytes, and breast cancer. *Cancers (Basel)* **14**, 3649. https://doi.org/10.3390/cancers14153649 (2022).
3. Eliassen, A. H. et al. Plasma 25-hydroxyvitamin D and risk of breast cancer in women followed over 20 years. *Cancer Res.* **76**, 5423–5430. https://doi.org/10.1158/0008-5472.CAN-16-0353 (2016).
4. Mohr, S. B., Gorham, E. D., Kim, J., Hofflich, H. & Garland, C. F. Meta-analysis of vitamin D sufficiency for improving survival of patients with breast cancer. *Anticancer Res.* **34**, 1163–6 (2014).
5. Chen, P. et al. Meta-analysis of vitamin D, calcium and the prevention of breast cancer. *Breast Cancer Res. Treat.* **121**, 469–477. https://doi.org/10.1007/s10549-009-0593-9 (2010).
6. Vrieling, A. et al. Serum 25-hydroxyvitamin D and postmenopausal breast cancer survival: a prospective patient cohort study. *Breast Cancer Res.* **13**, R74. https://doi.org/10.1186/BCR2920 (2011).
7. Song, D. et al. Vitamin D intake, blood vitamin D levels, and the risk of breast cancer: a dose-response meta-analysis of observational studies. *Aging (Albany NY)* **11**, 12708–12732. https://doi.org/10.18632/AGING.102597 (2019).
8. Zhou, L., Chen, B., Sheng, L. & Turner, A. The effect of vitamin D supplementation on the risk of breast cancer: A trial sequential meta-analysis. *Breast Cancer Res. Treat.* https://doi.org/10.1007/S10549-020-05669-4 (2020).
9. Prentice, R. L. et al. Health risks and benefits from calcium and vitamin D supplementation: Women's Health Initiative clinical trial and cohort study. *Osteoporos Int.* **24**, 567–580. https://doi.org/10.1007/s00198-012-2224-2 (2013).
10. Manson, J. A. E., Bassuk, S. S. & Buring, J. E. Principal results of the VITamin D and OmegA-3 TriaL (VITAL) and updated meta-analyses of relevant vitamin D trials. *J. Steroid Biochem. Mol. Biol.* https://doi.org/10.1016/J.JSBMB.2019.105522 (2020).
11. Scragg, R. The vitamin D assessment (ViDA) study - design and main findings. *J. Steroid Biochem. Mol. Biol.* https://doi.org/10.1016/J.JSBMB.2019.105562 (2020).
12. Virtanen, J. K. et al. Vitamin D supplementation and prevention of cardiovascular disease and cancer in the Finnish vitamin D trial: A randomized controlled trial. *Am. J. Clin. Nutr.* **115**, 1300–1310. https://doi.org/10.1093/AJCN/NQAB419 (2022).
13. Matilainen, J. M., Malinen, M., Turunen, M. M., Carlberg, C. & Väisänen, S. The number of vitamin D receptor binding sites defines the different vitamin D responsiveness of the CYP24 gene in malignant and normal mammary cells. *J. Biol. Chem.* **285**, 24174–83. https://doi.org/10.1074/jbc.M110.124073 (2010).
14. Dennis, C. et al. Local production of active vitamin D3 metabolites in breast cancer cells by CYP24A1 and CYP27B1. *J. Steroid Biochem. Mol. Biol.* **232**, 106331. https://doi.org/10.1016/J.JSBMB.2023.106331 (2023).
15. Lopes, N. et al. Alterations in vitamin D signalling and metabolic pathways in breast cancer progression: A study of VDR, CYP27B1 and CYP24A1 expression in benign and malignant breast lesions vitamin D pathways unbalanced in breast lesions. *BMC Cancer* **10**, 483. https://doi.org/10.1186/1471-2407-10-483 (2010).
16. Welsh, J. Function of the vitamin D endocrine system in mammary gland and breast cancer. *Mol. Cell Endocrinol.* **453**, 88–95. https://doi.org/10.1016/j.mce.2017.04.026 (2017).
17. Ditsch, N. et al. The association between vitamin D receptor expression and prolonged overall survival in breast cancer. *J. Histochem. Cytochem.* **60**, 121–129. https://doi.org/10.1369/0022155411429155 (2012).
18. Al-Azhri, J. et al. Tumor expression of vitamin D receptor and breast cancer histopathological characteristics and prognosis. *Clin. Cancer Res.* **23**, 97–103. https://doi.org/10.1158/1078-0432.CCR-16-0075 (2017).
19. Huss, L. et al. Vitamin D receptor expression in invasive breast tumors and breast cancer survival. *Breast Cancer Res.* **21**, 84. https://doi.org/10.1186/s13058-019-1169-1 (2019).
20. Zinser, G. M. & Welsch, J. E. Vitamin D receptor status alters mammary gland morphology and tumorigenesis in MMTV-neu mice. *Carcinogenesis* **25**, 2361–2372. https://doi.org/10.1093/CARCIN/BGH271 (2004).

21. Williams, J. D. et al. Tumor autonomous effects of vitamin D deficiency promote breast cancer metastasis. *Endocrinology* **157**, 1341–1347. https://doi.org/10.1210/en.2015-2036 (2016).

22. Zhalehjoo, N., Shakiba, Y. & Panjehpour, M. Gene expression profiles of CYP24A1 and CYP27B1 in malignant and normal breast tissues. *Mol. Med. Rep.* **15**, 467–473. https://doi.org/10.3892/mmr.2016.5992 (2017).

23. Li J, Luco AL, Ochietti B, Fadhil I, Camirand A, Reinhardt TA, et al. Tumoral vitamin D synthesis by CYP27B1 1-α-hydroxylase delays mammary tumor progression in the PyMT-MMTV mouse model and its action involves NF-κB modulation. Endocrinology. 2016;157: 2204–2216. doi:https://doi.org/10.1210/en.2015-1824

24. Yang, L. & Zhang, Y. Tumor-associated macrophages: from basic research to clinical application. *J. Hematol. Oncol.* **10**, 58. https://doi.org/10.1186/S13045-017-0430-2 (2017).

25. Fu, L. Q. et al. The roles of tumor-associated macrophages in tumor angiogenesis and metastasis. *Cell Immunol.* **353**, 104119. https://doi.org/10.1016/J.CELLIMM.2020.104119 (2020).

26. Monkawa, T., Yoshida, T., Hayashi, M. & Saruta, T. Identification of 25-hydroxyvitamin D3 1alpha-hydroxylase gene expression in macrophages. *Kidney Int.* **58**, 559–568. https://doi.org/10.1046/J.1523-1755.2000.00202.X (2000).

27. Esteban, L., Vidal, M. & Dusso, A. 1α-Hydroxylase transactivation by γ-interferon in murine macrophages requires enhanced C/EBPβ expression and activation. *J. Steroid Biochem. Mol. Biol.* **89–90**, 131–137. https://doi.org/10.1016/j.jsbmb.2004.03.092 (2004).

28. Nygaard, R. H. et al. Metabolism of 25-Hydroxy-vitamin D in human macrophages is highly dependent on macrophage polarization. *Int. J. Mol. Sci.* **23**, 10943. https://doi.org/10.3390/IJMS231810943/S1 (2022).

29. Anisiewicz, A., Łabędź, N., Krauze, I. & Wietrzyk, J. Calcitriol in the presence of conditioned media from metastatic breast cancer cells enhances Ex vivo polarization of M2 alternative murine bone marrow-derived macrophages. *Cancers (Basel)* **12**, 3485. https://doi.org/10.3390/cancers12113485 (2020).

30. Anisiewicz, A., Pawlik, A., Filip-Psurska, B. & Wietrzyk, J. Differential Impact of calcitriol and its analogs on tumor stroma in young and aged ovariectomized mice bearing 4T1 mammary gland cancer. *Int. J. Mol. Sci.* **21**, 6359. https://doi.org/10.3390/ijms21176359 (2020).

31. Anisiewicz, A. et al. Unfavorable effect of calcitriol and its low-calcemic analogs on metastasis of 4T1 mouse mammary gland cancer. *Int. J. Oncol.* **52**, 103–126. https://doi.org/10.3892/ijo.2017.4185 (2017).

32. Anisiewicz, A. et al. Vitamin d metabolite profile in cholecalciferol-or calcitriol-supplemented healthy and mammary gland tumor-bearing mice. *Nutrients* **12**, 1–28. https://doi.org/10.3390/nu12113416 (2020).

33. Stachowicz-Suhs, M. et al. Calcitriol promotes M2 polarization of tumor-associated macrophages in 4T1 mouse mammary gland cancer via the induction of proinflammatory cytokines. *Sci. Rep.* **14**, 3778. https://doi.org/10.1038/s41598-024-54433-x (2024).

34. Łabędź, N. et al. Dual effect of vitamin D3 on breast cancer-associated fibroblasts. *BMC Cancer* **24**, 209. https://doi.org/10.1186/s12885-024-11961-z (2024).

35. Lowry, O.H., Rosebrough, N.J., Farr, A.L., & Randall, R.J. Protein measurement with the folin phenol reagent.. *J. Biol. Chem.* **193**, 265–275. https://doi.org/10.1016/S0021-9258(19)52451-6 (1951).

36. Peterson, G. L. Review of the Folin phenol protein quantitation method of Lowry, Rosebrough, Farr and Randall. *Anal. Biochem.* **100**, 201–220. https://doi.org/10.1016/0003-2697(79)90222-7 (1979).

37. Wasnik, S. et al. 1,25-Dihydroxyvitamin D suppresses M1 macrophages and promotes M2 differentiation at bone injury sites. *JCI Insight.* https://doi.org/10.1172/JCI.INSIGHT.98773 (2018).

38. Guo, Y. et al. Effect of 1α,25(OH)2D3-Treated M1 and M2 macrophages on cell proliferation and Migration ability in Ovarian Cancer. *Nutr. Cancer* **74**, 2632–2643. https://doi.org/10.1080/01635581.2021.2014903 (2022).

39. Du, L. et al. KDM6B regulates M2 polarization of macrophages by modulating the stability of nuclear β-catenin. *Biochim. Biophys. Acta - Mol. Basis Dis.* **1869**, 166611. https://doi.org/10.1016/J.BBADIS.2022.166611 (2023).

40. Zhang, Y. et al. VDR status arbitrates the prometastatic effects of tumor-associated macrophages. *Mol. Cancer Res.* **12**, 1181–91. https://doi.org/10.1158/1541-7786.MCR-14-0036 (2014).

41. de Lyra, E.C., da Silva, I.A., Katayama, M.L.H., Brentani, M.M., Nonogaki, S., Góes, J.C.S, et al. 25(OH)D3 and 1,25(OH)2D3 serum concentration and breast tissue expression of 1α-hydroxylase, 24-hydroxylase and Vitamin D receptor in women with and without breast cancer. *J. Steroid Biochem. Mol. Biol.* **100**, 184–192 (2006).

42. Gunaydin, G. CAFs interacting with TAMs in tumor microenvironment to enhance tumorigenesis and immune evasion. *Front. Oncol.* **11**, 2669. https://doi.org/10.3389/FONC.2021.668349/BIBTEX (2021).

43. Roszer, T. Understanding the mysterious M2 macrophage through activation markers and effector mechanisms. *Mediators Inflamm.* **2015**, e816460. https://doi.org/10.1155/2015/816460 (2015).

44. DeNardo, D. G. & Ruffell, B. Macrophages as regulators of tumor immunity and immunotherapy. *Nat. Rev. Immunol.* **19**, 369. https://doi.org/10.1038/S41577-019-0127-6 (2019).

45. Pan, Y., Yu, Y., Wang, X. & Zhang, T. Tumor-associated macrophages in tumor immunity. *Front. Immunol.* https://doi.org/10.3389/FIMMU.2020.583084 (2020).

46. Mantovani, A. et al. The chemokine system in diverse forms of macrophage activation and polarization. *Trends Immunol.* **25**, 677–686. https://doi.org/10.1016/J.IT.2004.09.015 (2004).

47. Ambarus, C. A. et al. Systematic validation of specific phenotypic markers for in vitro polarized human macrophages. *J. Immunol. Methods* **375**, 196–206. https://doi.org/10.1016/J.JIM.2011.10.013 (2012).

48. Miyasato, Y. et al. High density of CD204-positive macrophages predicts worse clinical prognosis in patients with breast cancer. *Cancer Sci.* **108**, 1693–1700. https://doi.org/10.1111/CAS.13287 (2017).

49. Xiao, Y. et al. CD44-Mediated poor prognosis in glioma is Associated with M2-Polarization of Tumor-Associated macrophages and Immunosuppression. *Front. Surg.* **8**, 785. https://doi.org/10.3389/FSURG.2021.775194/BIBTEX (2022).

50. Rhee, I. Diverse macrophages polarization in tumor microenvironment. *Arch. Pharm. Res.* **39**, 1588–1596. https://doi.org/10.1007/S12272-016-0820-Y (2016).

51. Lawrence, T. & Natoli, G. Transcriptional regulation of macrophage polarization: enabling diversity with identity. *Nat. Rev. Immunol.* **11**, 750–761. https://doi.org/10.1038/NRI3088 (2011).

52. Kainulainen, K. et al. M1 macrophages induce protumor inflammation in melanoma cells through TNFR-NF-κB signaling. *J. Invest. Dermatol.* **142**, 3041-3051.e10. https://doi.org/10.1016/J.JID.2022.04.024 (2022).

53. Tiainen S, Tumelius R, Rilla K, Hämäläinen K, Tammi M, Tammi R, et al. High numbers of macrophages, especially M2-like (CD163-positive), correlate with hyaluronan accumulation and poor outcome in breast cancer. Histopathology. 2015;66: 873–883. doi:https://doi.org/10.1111/HIS.12607

54. Zhao, X., Qu, J., Sun, Y., Wang, J., Liu, X., & Wang, F., et al. Prognostic significance of tumor-associated macrophages in breast cancer: a meta-analysis of the literature. *Oncotarget. Impact J.* 2017. https://doi.org/10.18632/oncotarget.15736

55. Klingen, T. A., Chen, Y., Aas, H., Wik, E. & Akslen, L. A. Tumor-associated macrophages are strongly related to vascular invasion, non-luminal subtypes, and interval breast cancer. *Hum. Pathol.* **69**, 72–80. https://doi.org/10.1016/J.HUMPATH.2017.09.001 (2017).

56. Zhang, W. J. et al. Tumor-associated macrophages correlate with phenomenon of epithelial-mesenchymal transition and contribute to poor prognosis in triple-negative breast cancer patients. *J. Surg. Res.* **222**, 93–101. https://doi.org/10.1016/J.JSS.2017.09.035 (2018).

57. Moeenrezakhanlou, A., Nandan, D., Shephard, L. & Reiner, N. E. 1α,25-Dihydroxycholecalciferol activates binding of CREB to a CRE site in the *CD14* promoter and drives promoter activity in a phosphatidylinositol-3 kinase-dependent manner. *J. Leukoc Biol.* **81**, 1311–1321. https://doi.org/10.1189/jlb.1106681 (2007).

58. Moeenrezakhanlou, A., Shephard, L., Lam, L. & Reiner, N. E. Myeloid cell differentiation in response to calcitriol for expression *CD11b* and *CD14* is regulated by myeloid zinc finger-1 protein downstream of phosphatidylinositol 3-kinase. *J. Leukoc Biol.* **84**, 519–528. https://doi.org/10.1189/jlb.1207833 (2008).
59. Longtine, M. S. et al. Calcitriol regulates immune genes CD14 and CD180 to modulate LPS responses in human trophoblasts. *Reproduction* **154**, 735–744. https://doi.org/10.1530/REP-17-0183 (2017).
60. Koli, K. & Keski-Oja, J. 1,25-Dihydroxyvitamin D3 enhances the expression of transforming growth factor beta 1 and its latent form binding protein in cultured breast carcinoma cells. *Cancer Res.* **55**, 1540–6 (1995).
61. Bajbouj, K. et al. Vitamin D exerts significant Antitumor effects by suppressing vasculogenic mimicry in breast cancer cells. *Front. Oncol.* **12**, 918340. https://doi.org/10.3389/FONC.2022.918340/BIBTEX (2022).
62. Pawlik, A. et al. Calcitriol and its analogs establish the Immunosuppressive Microenvironment that drives metastasis in 4T1 mouse mammary gland Cancer. *Int. J. Mol. Sci.* **19**, 2116. https://doi.org/10.3390/IJMS19072116 (2018).
63. Gratchev, A. TGF-β signalling in tumour associated macrophages. *Immunobiology* **222**, 75–81. https://doi.org/10.1016/J.IMBIO.2015.11.016 (2017).
64. Zhang, F. et al. TGF-β induces M2-like macrophage polarization via SNAIL-mediated suppression of a pro-inflammatory phenotype. *Oncotarget.* **7**, 52294–52306. https://doi.org/10.18632/ONCOTARGET.10561 (2016).
65. Chang, P. L., Ridall, A. L. & Prince, C. W. Calcitriol regulation of osteopontin expression in mouse epidermal cells. *Endocrinology* **135**, 863–9. https://doi.org/10.1210/endo.135.3.8070379 (1994).
66. Yan, Z., Hu, X., Tang, B. & Deng, F. Role of osteopontin in cancer development and treatment. *Heliyon* **9**, e21055. https://doi.org/10.1016/J.HELIYON.2023.E21055 (2023).
67. Icer, M. A. & Gezmen-Karadag, M. The multiple functions and mechanisms of osteopontin. *Clin. Biochem.* **59**, 17–24. https://doi.org/10.1016/J.CLINBIOCHEM.2018.07.003 (2018).
68. So, J. Y. et al. A novel gemini vitamin D analog represses the expression of a stem cell marker CD44 in breast cancer. *Mol. Pharmacol.* **79**, 360–367. https://doi.org/10.1124/mol.110.068403 (2011).
69. Imrich, S., Hachmeister, M. & Gires, O. EpCAM and its potential role in tumor-initiating cells. *Cell Adh. Migr.* **6**, 30–38. https://doi.org/10.4161/CAM.18953 (2012).
70. Spizzo, G. et al. High Ep-CAM expression is associated with poor prognosis in node-positive breast cancer. *Breast Cancer Res. Treat.* **86**, 207–213. https://doi.org/10.1023/B:BREA.0000036787.59816.01 (2004).
71. Benko, G., Spajić, B., Krušlin, B. & Tomas, D. Impact of the EpCAM expression on biochemical recurrence-free survival in clinically localized prostate cancer. *Urol. Oncol.* **31**, 468–474. https://doi.org/10.1016/J.UROLONC.2011.03.007 (2013).
72. Spizzo, G. et al. Overexpression of epithelial cell adhesion molecule (Ep-CAM) is an independent prognostic marker for reduced survival of patients with epithelial ovarian cancer. *Gynecol. Oncol.* **103**, 483–488. https://doi.org/10.1016/J.YGYNO.2006.03.035 (2006).
73. Eslami, -S. Z., Cortés-Hernández, L. E. & Alix-Panabières, C. Epithelial cell adhesion molecule: An anchor to isolate clinically relevant circulating tumor cells. *Cells* **9**, 1–17. https://doi.org/10.3390/CELLS9081836 (2020).
74. Liu, Y. et al. Understanding the versatile roles and applications of EpCAM in cancers: From bench to bedside. *Exp. Hematol. Oncol.* https://doi.org/10.1186/S40164-022-00352-4 (2022).
75. Xie, J. et al. Yes-associated protein regulates the hepatoprotective effect of vitamin D receptor activation through promoting adaptive bile duct remodeling in cholestatic mice. *J. Pathol.* **255**, 95–106. https://doi.org/10.1002/PATH.5750 (2021).
76. Lu, J., Liang, T., Li, P. & Yin, Q. Regulatory effects of IRF4 on immune cells in the tumor microenvironment. *Front. Immunol.* https://doi.org/10.3389/FIMMU.2023.1086803 (2023).
77. Zhu, X. et al. 1,25–Dihydroxyvitamin D regulates macrophage polarization and ameliorates experimental inflammatory bowel disease by suppressing miR-125b. *Int. Immunopharmacol.* **67**, 106–118. https://doi.org/10.1016/J.INTIMP.2018.12.015 (2019).
78. Gauzzi, M. C. et al. IRF-4 expression in the human myeloid lineage: up-regulation during dendritic cell differentiation and inhibition by 1alpha,25-dihydroxyvitamin D3. *J. Leukoc Biol.* **77**, 944–947. https://doi.org/10.1189/JLB.0205090 (2005).
79. Carreras E, Turner S, Frank MB, Knowlton N, Osban J, Centola M, et al. Estrogen receptor signaling promotes dendritic cell differentiation by increasing expression of the transcription factor IRF4. Blood. 2010;115: 238–246. doi:https://doi.org/10.1182/blood-2009-08-236935
80. Denger, S. et al. Transcriptome profiling of estrogen-regulated genes in human primary osteoblasts reveals an osteoblast-specific regulation of the insulin-like growth factor binding protein 4 Gene. *Mol. Endocrinol.* **22**, 361–379. https://doi.org/10.1210/me.2007-0292 (2008).
81. Yang, J., Zhang, L., Yu, C., Yang, X.-F. & Wang, H. Monocyte and macrophage differentiation: Circulation inflammatory monocyte as biomarker for inflammatory diseases. *Biomark. Res.* **2**, 1. https://doi.org/10.1186/2050-7771-2-1 (2014).
82. Bauer, S. R., Hankinson, S. E., Bertone-Johnson, E. R. & Ding, E. L. Plasma vitamin d levels, menopause, and risk of breast cancer:dose-response meta-analysis of prospective studies. *Med. (United States)* **92**, 123–131. https://doi.org/10.1097/MD.0b013e3182943bc2 (2013).
83. O'Brien, K. M., Sandler, D. P., Taylor, J. A. & Weinberg, C. R. Serum vitamin D and risk of breast cancer within five years. *Environ. Health Perspect.* https://doi.org/10.1289/EHP943 (2017).
84. Xu, S. et al. Calcitriol inhibits migration and invasion of renal cell carcinoma cells by suppressing Smad2/3-, STAT3- and β-catenin-mediated epithelial-mesenchymal transition. *Cancer Sci.* **111**, 59–71. https://doi.org/10.1111/CAS.14237 (2020).
85. Xing, W. Y. et al. Calcitriol inhibits lipopolysaccharide-induced proliferation, migration and invasion of prostate cancer cells through suppressing STAT3 signal activation. *Int. Immunopharmacol.* **82**, 106346. https://doi.org/10.1016/J.INTIMP.2020.106346 (2020).
86. Łabędź, N. et al. Modulation of fibroblast activity via vitamin D3 is dependent on tumor type—studies on mouse mammary gland cancer. *Cancers (Basel)* **14**, 4585. https://doi.org/10.3390/cancers14194585 (2022).
87. Mego, M. et al. Vitamin D and circulating tumor cells in primary breast cancer. *Front. Oncol.* https://doi.org/10.3389/FONC.2022.950451/FULL (2022).

Acknowledgements

Author contributions

M.S.-S. conducted all the research and contributed to the writing of the manuscript. N.Ł. obtained tissues from patients, participated in cell isolation, and contributed to writing the manuscript. M.M., D.K., and B.F.-P. were involved in tissue analysis and interpreting the results. A.M. and R.M. collected tissues from patients, obtained clinical data, and participated in interpreting these data. J.W. analyzed and interpreted the patient data and was a major contributor to writing the manuscript. All authors have read and approved the final manuscript.

Funding

funders had no role in the design of the study; in the collection, analyses, or interpretation of the data; in the writing of the manuscript; or in the decision to publish the results.

Declarations

Ethics approval and consent to participate
For research on tissues from patients diagnosed at the Lower Silesian Center of Oncology, Pulmonology, and Hematology (February 2019 to December 2020), consent was obtained from the Bioethical Committee at the Medical University in Wrocław, Poland (approval numbers 603/2018 and 855/2019). Studies were carried out in line with the ethical standards of the national and institutional research committee and with the latest version of the Declaration of Helsinki. All patients signed an informed consent form to participate in the study.

Competing interests
The authors declare no competing interests.

Additional information
Supplementary Information The online version contains supplementary material available at https://doi. org/10.1038/s41598-024-73152-x.

Correspondence and requests for materials should be addressed to J.W.

Reprints and permissions information is available at www.nature.com/reprints.

Publisher's note Springer Nature remains neutral with regard to jurisdictional claims in published maps and institutional affiliations.